



Assessment of basin-scale groundwater potentiality mapping in drought-prone upper Dwarakeshwar River basin, West Bengal, India, using GIS-based AHP techniques

Ujjal Senapati¹ · Tapan Kumar Das²

Received: 9 September 2020 / Accepted: 12 May 2021 / Published online: 24 May 2021
© Saudi Society for Geosciences 2021

Abstract

Sustainable use of groundwater is essential in any region to increase long-term agricultural sustainability as well as to maintain the pace of socio-economic development of the region. Groundwater is a most vital and valuable natural resource for ecosystems and communities in the drought-prone western part of West Bengal, India. The intensity of agriculture in drought-prone areas has resulted in the expansion of groundwater. The current study has been conducted in a semi-arid upper Dwarakeshwar River basin which is basically a meteorological as well as agricultural drought-prone and agro-economy-based region. The current paper attempts to illustrate the areas of groundwater potentiality by using Analytical Hierarchy Process (AHP) and Geographic Information System (GIS). Appropriate weight has been determined for each factor and their subclasses on the basis of their relative importance by using the AHP technique. The final output map has been integrated by using total twelve sets of groundwater influencing thematic layers, namely: aquifer media, mean annual groundwater level, lithology, land use and land cover, rainfall, drainage density, soil drainage, soil texture, Normalized Difference Vegetation Index (NDVI), elevation, curvature, and slope. It has been classified into five zones: very poor, poor, moderate, well, and excellent covering an area of 256.87 km² (13.38%), 581.79 km² (30.30%), 607.91 km² (31.66%), 381.58 km² (19.87%), and 91.36 km² (4.76%), respectively, and finally, results have been validated with the help of mean annual groundwater level data of 50 dug wells through the Receiver Operating Characteristic (ROC) curve. The result of Area Under Curve (AUC) value is 0.871 that indicates 87.1% accuracy and reliability for better planning, management, and resource development in an effective way.

Keywords Groundwater potentiality · Thematic layers · AHP · GIS · ROC · Dwarakeshwar River

Introduction

Groundwater is a common and most significant source of drinking water, which also provides for irrigation worldwide (Gleick 1993; Hellegers et al. 2001; Wang et al. 2012; Mukherjee et al. 2012; Pfeiffer and Lin 2014; Kolanuvada et al. 2019; Jasrotia et al. 2019; Kadam et al. 2020).

Approximately 1.5 billion people are dependent on groundwater, and a population of 2.53 billion are living in highly water-stressed parts of the world (Shen et al. 2008; Shen et al. 2014). In arid and semi-arid regions, groundwater is one of the most essential and valuable natural resources (Razandi et al. 2015; Mukherjee et al. 2012). Groundwater is the only source of long-lived water supply in dry, drought-prone areas of the world, and nowadays, groundwater is being increasingly exploited for public supply of drinking and agricultural purposes (Calow et al. 1997; Peters et al. 2005). During drought, the performance of groundwater becomes increasingly significant (White et al. 1999; Peters et al. 2005). It has been shown that the characteristics of the groundwater systems change in drought-prone regions due to the excessive use of groundwater (Peters et al. 2003). In developing countries such as India, groundwater plays a key role in turning the wheel of development, especially in the agrarian economy (Bhunia et al. 2012). According to the National

Responsible Editor: Broder J. Merkel

✉ Ujjal Senapati
senapati.ujjal2012@gmail.com

¹ Department of Geography, Cooch Behar Panchanan Barma University, Vivekananda Rd, Cooch Behar, West Bengal 736101, India

² Department of Geography, Cooch Behar College, Cooch Behar, West Bengal, India

Institute of Hydrology (NIH), India is the world's largest groundwater user (Kumar and Krishna 2016). In India, more than 90% of rural and more than 30% of the urban population are dependent on groundwater for their livelihood (Agarwal and Garg 2016; Patra et al. 2018). Another research shows that currently 85% of India's rural population meet their drinking and domestic water needs from groundwater (Kadam et al. 2020). Currently, many states of India are suffering from severe groundwater crisis due to the rapidly growing population and increasing inhabitants' area, agriculture, and rapid industrialization. So it has resulted in continued abstraction, degradation, and depletion of groundwater (Pande et al. 2017; Patra et al. 2018; Das and Mukhopadhyay 2018; Kadam et al. 2020). The total annual groundwater availability of West Bengal is 22.56 Billion Cubic Meter (BCM) and the gross draft used is 10.91 BCM (Rudra et al. 2017). The availability of groundwater is limited in hard cliffs like the Red and Latic zones (Chowdhury et al. 2009; Thivya et al. 2014; Shekhar and Pandey 2015).

The western districts of West Bengal, mainly Purulia, Bankura, Jhargram, Paschim Midnapore, and Bribhnum are recurrently facing an irregular deficit of annual rainfall, thus being repeatedly affected by drought. During the summer months, most surface water sources such as ponds and streams dry up completely and stand as the only alternative to the groundwater supply (Thapa et al. 2017; Ghosh and Jana 2017; Roy et al. 2020). The study area falls between Purulia and Bankura districts. This region is recognized as a historically drought-prone region due to its undulating terrain capped which generates huge runoff, followed by a quick return of water into the atmosphere owing to higher evaporation rate (Mukherjee and Singh 2020). Though this region receives high amount of rainfall (1400 mm), 90% of rainfall happens in the months of June to September (Ghosh and Jana 2017). Acute water shortage has been observed in this region mainly during the summer season (pre-monsoon season). As the district is drought-prone, farmers are dependent on rainfall during the monsoon for their agricultural activities. This study area faced severe meteorological as well as agricultural drought several times in the recent decade (Das et al. 2013; Palchaudhuri and Biswas 2020; Bhunia et al. 2020). In recent years (2000–2016), this region experienced agricultural drought conditions in 2002, 2010, and 2015 (Palchaudhuri and Biswas 2020).

Different strategies which have been adopted by researchers to tackle these issues are Multi-Influencing Factor (MIF) (Magesh et al. 2012), frequency ratio (Elmahdy and Mohamed 2015; Guru et al. 2017), GIS-based Influencing Factor (IF) and Frequency Ratio (FR) techniques (Das and Pardeshi 2018), GIS-based Dempster-Shafer model (Mogaji et al. 2015), Logistic Regression (LR) (Pourtaghi and Pourghasemi 2014), Certainty Factor (CF) (Razandi et al. 2015), Weights-Of-Evidence (WOE) (Al-Abadi 2015; Tahmassebpour et al. 2016; Ghorbani Nejad

et al. 2017), Evidential Belief Function (EBF) (Pourghasemi and Beheshtirad 2015), Maximum Entropy (ME) (Rahmati et al. 2014), fuzzy logic (Ghayoumian et al. 2007), machine learning models like Artificial Neural Network (ANN) (Lee et al. 2012; Lee et al. 2018), Classification And Regression Tree (CART) and Boosted Regression Tree (BRT) (Naghbi and Pourghasemi 2015), numerical modeling and Decision Tree (DT) (Saghebian et al. 2014; Lee and Lee 2015), random forest model (Naghbi et al. 2016), multivariate adaptive regression spline model (Zabihi et al. 2016) etc. Groundwater is an unexposed and valuable natural resource, and therefore, it cannot be directly identified. Although various sets of methods are used to search for groundwater, its mapping is an extremely challenging task. Stratigraphy investigation, drilling test, and boring are the most commonly used methods for determining the groundwater level and the thickness of the aquifers, and for estimating the volume of present groundwater (Jha et al. 2010; Bera et al. 2021). However, these methods rely on heavy materials and are expensive and time-consuming in determining the availability of groundwater resources in an area (Patra et al. 2018).

Lithologically, Purulia and some parts of Bankura district are a hard rock terrain, and as a consequence of this, they have low primary porosity and permeability. The layer of soil overlying the hard rock terrain shows a maximum depth of 25 m and the retaining capacity of soil ranges from medium to low (Bera and Das 2021). Deep aquifer is rarely found in the entire Purulia district. In western part of Bankura, weathered residuum and fractures of granite are the main source of ground water with a depth of 30–60 m below ground level (Bhunia et al. 2020). In hard rock regions, the lack of reliable information and the complexity of the highly variable nature of the geological environment make it a relatively complex task (Guru et al. 2017). Over the past few decades, several studies have been conducted around the world to identify potential areas of groundwater using remote sensing and GIS (Ahmed II and Mansor 2018; Patra et al. 2018; Mageshkumar et al. 2019; Rehman et al. 2019; Rajasekhar et al. 2020; Bera et al. 2020). Remote sensing and GIS strategies plays an important role in identifying suitable sites for sustainable groundwater management. In this context, for the integration of GIS, RS method can be cited as an example of a process that converts and integrates geographic data and weight rankings for decision-making with AHP techniques (Sargaonkar et al. 2011).

In the present days, AHP multi-criteria techniques have been considered a standardized system to assess groundwater potentiality and has been applied by several researchers (Ferozu et al. 2018; Patra et al. 2018; Nithya et al. 2019; Rajasekhar et al. 2019; Arefin 2020a, b; Mukherjee and Singh 2020). The AHP method is a well-renowned tool largely used in multi-criteria technique which has been incorporated into the GIS-based suitability procedures, and the accuracy of this model is remarkably high (Bera et al. 2020; Biswas et al. 2020). The present study focuses on the identification of groundwater potential zone in the upper Dwarakeshwar River

basin, West Bengal, using AHP and GIS techniques for the management and planning of groundwater resources. It also helps to select the most suitable drilling location of new groundwater exploration wells. In addition, this method can widely be used for sustainable water resource management, groundwater exploration, and artificial recharge zone identification in different parts of the world, where similar kind of physio-climatic conditions are observed.

Study area

The upper part of the Dwarakeshwar River basin is situated in the central part of Purulia and Bankura districts. Geomorphologically, this river basin is a part of the “Chotanagpur Plateau” region. This river is rain-fed and flows from northwest to southeast (Roy et al. 2020). It is situated between 23° 08' 58.80" and 23° 31' 55.88" north latitudes and between 86° 30' 52.43" and 87° 09' 13.34" east longitudes

(Fig. 1). It has an area of 1934 km². The average temperature of this subtropical semi-arid region is 40–46°C in summer and about 7–11°C in winter. The recorded annual rainfall is around 1200–1400 mm. Eighty percent of the total rainfall occurs during the monsoon season and the rest of the twenty percent is raining during the pre and post-monsoon seasons. The terrain is characterized by hard rock plateaus, enclosing laterites, and flat sedimentary fields (Nag and Kundu 2016). Agriculture is the main source of livelihood in this drought-prone study area. Aus and aman paddy, pulses, mustard, and potato are the main crops of the study area.

Materials and methods

The potential groundwater mapping of upper Dwarakeshwar River basin consists of four main parts—(1) Spatial data have been collected which are directly or indirectly related to

Fig. 1 Location map of the study area. **a** India. **b** West Bengal (Bankura district is shown in yellow and Purulia district shown in blue color). **c** Spatial distribution of dug well and rainfall station of upper Dwarakeshwar River basin

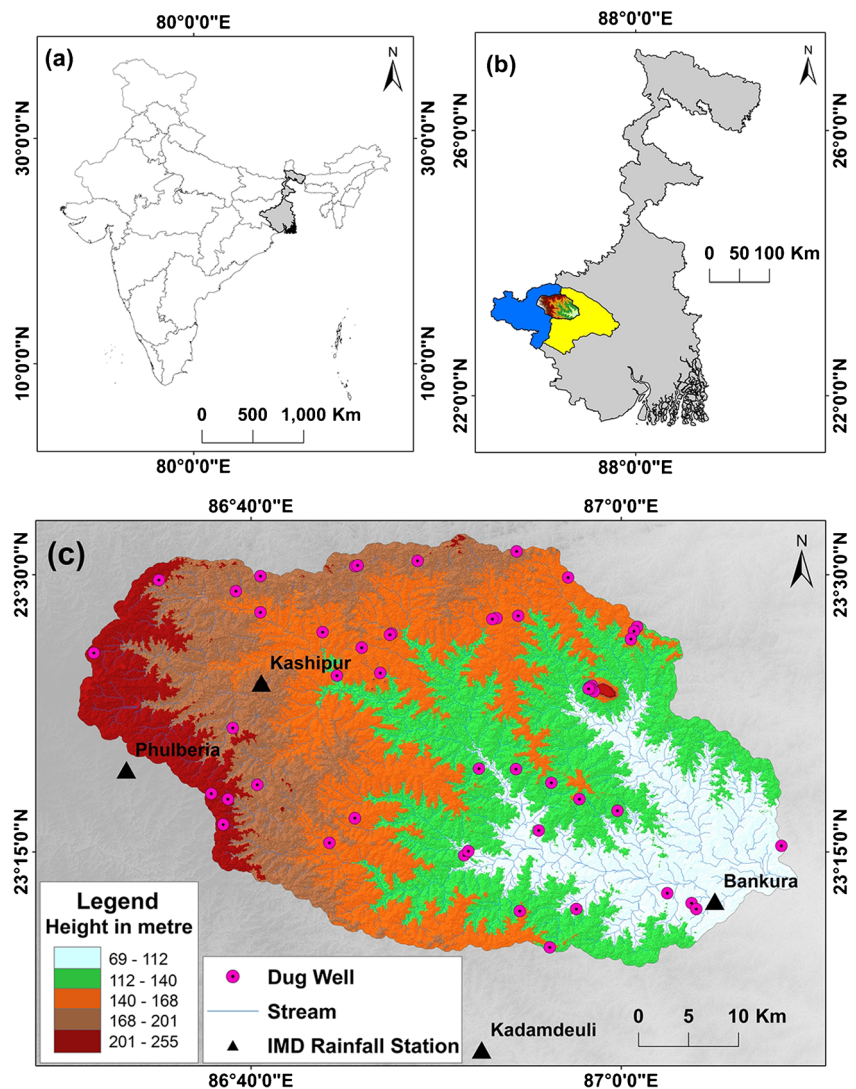
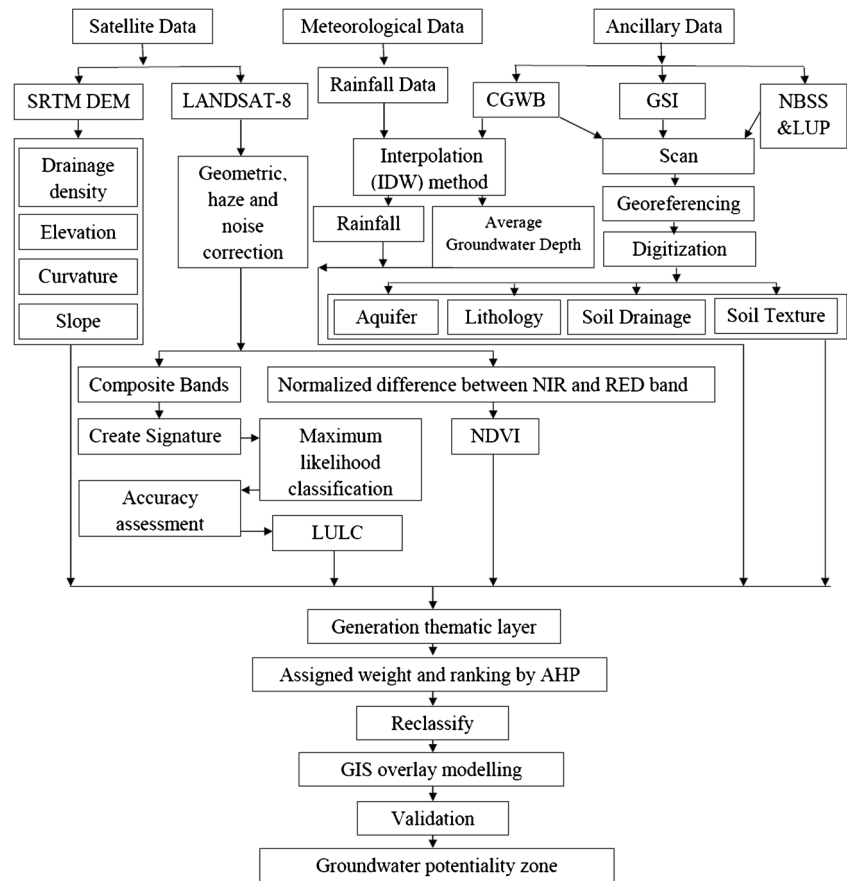


Fig. 2 Methodological flowchart of groundwater potential zone



groundwater potential. The description of these data and their main sources are shown in Table 1. (2) The collected data sets have been converted into thematic maps, using GIS software. The pixel sizes of all thematic layers have been resampled to 30 m. (3) The weights are calculated for related factors and their subclasses through AHP comparison matrix. (4) Finally, the groundwater potential map is prepared using the weighted overlay analysis method and it is further validated with the help of Receiver Operating Characteristic (ROC) curve.

The methodological flowchart in this study has been presented in Fig. 2 .

Preparation of thematic layers

The potential groundwater mapping of the upper Dwarakeshwar River basin has been determined using 12 thematic layers. The aquifer map was collected from the Central Ground Water Board (CGWB), Ministry of water Resources, Government of

Table 1 Data sources used for thematic layer preparation

Data	Source
Aquifer systems of India (scale—1:50,000)	Central Ground Water Board (CGWB), Ministry of water Resources, Government of India
Ground water data	Central Ground Water Board (CGWB), India, http://cgwb.gov.in/
Lithology (scale—1:50,000)	Geological Survey of India (GSI)
LANDSAT 8 (spatial resolution 30 m)	USGS earth explorer (LC08_L1TP_139044_20181220_20181227_01_T1)
SRTM DEM (spatial resolution 30 m)	USGS earth explorer (n23_e086_1arc_v3, n23_e087_1arc_v3)
Rainfall data	India Meteorological Department (IMD), Pune
Soil texture and drainage map (scale—1:50,000)	National Bureau of Soil Survey and Land Use planning (NBSS & LUP)

India. The lithology map was collected from the Geological Survey of India (GSI). The soil drainage and soil texture maps were obtained from the National Bureau of Soil Survey and Land Use Planning (NBSS & LUP). These maps were scanned and georeferenced using WGS 84 datum, UTM zone 45 N projection. The ArcGIS 10.3 software has been employed to digitize the maps intended for further analysis. The Average groundwater level map is prepared by the Inverse Distance-Weighted (IDW) interpolation method using seasonal point data, collected from the Central Ground Water Board (CGWB). The rainfall data has been collected from India Meteorological Department (IMD), Pune, and the rainfall map is prepared by the IDW interpolation method. The elevation, curvature, and slope, maps were prepared from the Shuttle Radar Topographic Mission (SRTM) Digital Elevation Model (DEM) having a resolution of 30 m. In ARC GIS 10.3 environment using the spatial analyst tools, firstly, the flow direction map followed by the flow accumulation map were performed, and finally, the streams are generated. Using line density tool, the drainage map is prepared. In this study, Normalized Difference Vegetation Index (NDVI) maps were prepared from Landsat 8 data. The NDVI is calculated using the following formula (Rouse et al. 1974):

$$NDVI = \frac{(NIR\ BAND - RED\ BAND)}{(NIR\ BAND + RED\ BAND)}$$

The land use and land cover map has been prepared from Landsat 8 OLI satellite imagery from earth explorer (<https://earthexplorer.usgs.gov/>) which further cross checked by field verification. It was pre-processed for noise and haze correction, and then, all bands were made composite. Classifications were created using the supervised classification method under the maximum likelihood classification tool of Arc GIS 10.3 software.

Analytical Hierarchy Process (AHP)

Analytical Hierarchy Process (AHP) is simple and widely used for multiple purposes, and it has a worldwide acceptance in multi-criterion decision making that was first introduced by Saaty (1980). The AHP method enables the estimate of percentage distribution in result judgment points with conditioning factors that affect the result. This method conducts a comparison matrix for the discretion of a decision sequence. Significant differences are disclosed in terms of percentage distribution in decision points (Nefeslioglu et al. 2013). The adoption of AHP, particularly for

qualitative performance data, is due to the fact that qualitative factors are often complicated and inconsistent. In addition, when compared to other multi-attribute decision methods, the user acceptability and consistency in the analysis given by the AHP methodology is strong, and precise calculations are carried out in the expert choice process, and it can be understood and measured very easily (Kumru and Kumru 2014). The AHP provides a framework for subjective decision-making processes, serves as a consistency checker and makes predictions about the implicit weights of assessment criteria, and enhances clarity and engagement among members of the decision-making team, resulting in a commitment to the preferred alternative (Kumru and Kumru 2014; Horňáková et al. 2019).

In the basin-scale study, potential areas of groundwater in the study area have been identified based on a total of twelve thematic layers with factors such as aquifer, average groundwater level, lithology, Land Use and Land Cover (LULC), rainfall, drainage density, soil drainage, soil texture, NDVI, elevation, curvature, and, slope. Then, weights are allocated to the thematic layers, based on their relative importance and influencing capacity in considering the probability of groundwater potentiality. The weightage is given on each parameter according to its relative importance. The Satty relative scale ranges from 1 to 9, where 1 denotes the trivial or equal significance and 9 denotes final choice or absolute significance which is used for the analytical decision-making, as shown in Table 2. The decision hierarchy is assigned as an off-diagonal relation of one-half of the value of each matrix in the even comparison matrix. The role of each factor independently evaluates on this pairwise comparison matrix (Table 3). Then, the normalized matrix of GWPZ is calculated (Table 4). The subclasses of each individual thematic raster layers have been given weights by using the pairwise comparison matrix and a relative rating of each subclass (Table 5). Consistency Ratio (CR) checked to determining either pairwise comparisons has been consistent or not. If CR < 0.10, it indicates acceptability of continuity, for recognizing the class weights. Otherwise, re-assessment of the concerning weights is done to avoid inconsistencies (Agarwal and Garg 2016; Bera et al. 2019). CR has been calculated from this following equation:

$$CR = \frac{CI}{RCI}$$

where CR = consistency ratio; CI = consistency index; RCI = random consistency index, and CI = consistency indexes have

Table 2 The Satty 9-point relative scale

Scale's	1	2	3	4	5	6	7	8	9
Degree of importance	Equal	Weak	Slight	Moderate	Quite	Very strong	Extreme	Very strongly extreme	Absolute

Table 3 Pairwise comparison matrix for all parameters

Parameter	AQ	MAGL	LI	LULC	RA	DD	SD	ST	NDVI	EL	CU	SL
Aquifer	1	2	3	4	5	5	6	6	7	8	8	9
Mean annual groundwater level	1/2	1	2	3	4	5	5	6	6	7	8	9
Lithology	1/3	1/2	1	2	3	4	5	5	6	6	7	8
Land use and land cover	1/4	1/3	1/2	1	2	3	4	5	5	6	6	7
Rainfall	1/5	1/4	1/3	1/2	1	2	3	4	5	6	6	7
Drainage density	1/5	1/5	1/4	1/3	1/2	1	2	3	4	5	5	6
Soil drainage	1/6	1/5	1/5	1/4	1/3	1/2	1	2	3	4	5	5
Soil texture	1/6	1/6	1/5	1/5	1/4	1/3	1/2	1	2	1	1	5
NDVI	1/7	1/6	1/6	1/5	1/5	1/4	1/3	1/2	1	2	3	4
Elevation	1/8	1/7	1/6	1/6	1/6	1/5	1/4	1	1/2	1	2	3
Curvature	1/8	1/8	1/7	1/6	1/6	1/5	1/5	1	1/3	1/2	1	2
Slope	1/9	1/9	1/8	1/7	1/7	1/6	1/5	1/5	1/4	1/3	1/2	1

been calculated from the following equation (Kumar and Krishna 2016).

$$CI = \frac{\lambda_{max} - n}{n - 1}$$

where CI is the consistency index; λ_{max} is the principal eigenvalue of the decision matrix, and n is the total number of factors. The principal eigenvalue (λ) has been calculated from the

equation given below (Agarwal and Garg 2016; Kumar and Krishna 2016).

$$\lambda_{max} = \frac{1}{n} \sum_{wi} \frac{(AW)_i}{wi}$$

where λ_{max} is the principal eigenvalue; W is eigenvector of λ_{max} ; and wi is the eigenvalue of weight value for ranking i. The value of the random consistency index (RCI) was obtained

Table 4 Normalized matrix of for all parameters

Parameter	Aquifer	Mean annual groundwater level	Lithology	Land use and land cover	Rainfall	Drainage density	Soil drainage	Soil texture	NDVI	Elevation	Curvature	Slope	Weights
Aquifer	0.3011	0.3849	0.3711	0.3345	0.2983	0.2309	0.2183	0.1729	0.1746	0.1708	0.1524	0.1364	0.2455
Mean annual groundwater level	0.1506	0.1925	0.2474	0.2508	0.2387	0.2309	0.1819	0.1729	0.1497	0.1495	0.1524	0.1364	0.1878
Lithology	0.1004	0.0962	0.1237	0.1672	0.179	0.1848	0.1819	0.1441	0.1497	0.1281	0.1333	0.1212	0.1425
Land use and land cover	0.0753	0.0642	0.0618	0.0836	0.1193	0.1386	0.1455	0.1441	0.1247	0.1281	0.1143	0.1061	0.1088
Rainfall	0.0602	0.0481	0.0412	0.0418	0.0597	0.0924	0.1092	0.1153	0.1247	0.1281	0.1143	0.1061	0.0868
Drainage density	0.0602	0.0385	0.0309	0.0279	0.0298	0.0462	0.0728	0.0865	0.0998	0.1068	0.0952	0.0909	0.0655
Soil drainage	0.0502	0.0385	0.0247	0.0209	0.0199	0.0231	0.0364	0.0576	0.0748	0.0854	0.0952	0.0758	0.0502
Soil texture	0.0502	0.0321	0.0247	0.0167	0.0149	0.0154	0.0182	0.0288	0.0499	0.0214	0.019	0.0758	0.0306
NDVI	0.043	0.0321	0.0206	0.0167	0.0119	0.0115	0.0121	0.0144	0.0249	0.0427	0.0571	0.0606	0.029
Elevation	0.0376	0.0275	0.0206	0.0139	0.0099	0.0092	0.0091	0.0288	0.0125	0.0214	0.0381	0.0455	0.0228
Curvature	0.0376	0.0241	0.0177	0.0139	0.0099	0.0092	0.0073	0.0288	0.0083	0.0107	0.019	0.0303	0.0181
Slope	0.0335	0.0214	0.0155	0.0119	0.0085	0.0077	0.0073	0.0058	0.0062	0.0071	0.0095	0.0152	0.0125

Principal eigenvalue = 13.047306; consistency ratio (CR) = 0.062017

Table 5 Normalize weight assignments for all subcategories by AHP techniques.

Parameter	Subclasses	1	2	3	4	5	6	7	CR	Weights
Aquifer	Older alluvium	1	2	3	5	7	9		0.009261	0.414789
	Older alluvium, sand, and silt	1/2	1	2	3	5	7			0.254692
	Laterite	1/3	1/2	1	2	3	5			0.153233
	Schist	1/5	1/3	1/2	1	2	3			0.089637
	Banded Gneissic Complex	1/7	1/5	1/3	1/2	1	2			0.054036
	Basic intrusives	1/9	1/7	1/5	1/3	1/2	1			0.033613
Mean annual groundwater level	2.13–3.92	1	3	5	7	9			0.052763	0.512808
	3.93–4.45	1/3	1	3	5	7				0.261513
	4.46–4.97	1/5	1/3	1	3	5				0.128978
	4.98–6.05	1/7	1/5	1/3	1	3				0.063371
	6.05–8.82	1/9	1/7	1/5	1/3	1				0.033331
Lithology	Tertiary to Quarternary	1	2	3	4				0.011357	0.467295
	Pleistocene to Recent	1/2	1	2	3					0.277181
	Paleozoic to Jurassic	1/3	1/2	1	2					0.160089
	Archaean to Tertiary	1/4	1/3	1/2	1					0.095435
Land use and land cover	Water bodies	1	2	3	4	5			0.01514	0.418534
	Natural vegetation	1/2	1	2	3	4				0.262519
	Agricultural land	1/3	1/2	1	2	3				0.159926
	Fallow land	1/4	1/3	1/2	1	2				0.097255
	Settlement	1/5	1/4	1/3	1/2	1				0.061766
Rainfall	1585–1631	1	3	4	6	7			0.057679	0.485101
	1540–1584	1/3	1	3	4	6				0.261929
	1499–1539	1/4	1/3	1	3	4				0.138849
	1454–1498	1/6	1/4	1/3	1	3				0.073692
	1398–1453	1/7	1/6	1/4	1/3	1				0.04043
Drainage density	0.0021–0.72	1	2	4	5	7			0.016312	0.457232
	0.73–1.1	1/2	1	2	4	5				0.266641
	1.2–1.4	1/4	1/2	1	2	4				0.147535
	1.5–1.9	1/5	1/4	1/2	1	2				0.080526
	2–3.6	1/7	1/5	1/4	1/2	1				0.048066
Soil drainage	Excessive	1	2	3	5	7	8	9	0.019654	0.382138
	Somewhat excessive	1/2	1	2	3	5	7	8		0.247937
	Well	1/3	1/2	1	2	3	5	7		0.157006
	Mod. well	1/5	1/3	1/2	1	2	3	5		0.094868
	Imperfect well	1/7	1/5	1/3	1/2	1	2	3		0.056972
	Imperfect mod	1/8	1/7	1/5	1/3	1/2	1	2		0.03639
	Imperfect	1/9	1/8	1/7	1/5	1/3	1/2	1		0.02469
Soil texture	Sandy-loamy group	1	2	3	5	7			0.006237	0.444648
	Sandy-clay group	1/2	1	2	3	5				0.261921
	Loamy group	1/3	1/2	1	2	3				0.152359
	Gravelly group	1/5	1/3	1/2	1	2				0.08868
	Clay group	1/7	1/5	1/3	1/2	1				0.052392
NDVI	0.201 to 0.387	1	3	5	7				0.025134	0.569273
	0.101 to 0.2	1/3	1	3	5					0.264284
	0.001 to 0.1	1/5	1/3	1	2					0.105522
	– 0.134 to 0	1/7	1/5	1/2	1					0.060921
Elevation	69–112	1	2	3	4	5			0.01514	0.418534
	113–140	1/2	1	2	3	4				0.262519
	141–168	1/3	1/2	1	2	3				0.159926

Table 5 (continued)

Parameter	Subclasses	1	2	3	4	5	6	7	CR	Weights
Curvature	169–201	1/4	1/3	1/2	1	2			0.040191	0.097255
	202–255	1/5	1/4	1/3	1/2	1				0.061766
	Concave	1	3	5						0.636982
	Flat	1/3	1	3						0.25829
	Convex	1/5	1/3	1						0.104729
Slope	0–1	1	2	4	7	9			0.007106	0.482633
	1.1–3	1/2	1	2	4	7				0.268298
	3.1–5	1/4	1/2	1	2	4				0.138139
	5.1–7	1/7	1/4	1/2	1	2				0.070782
	> 7	1/9	1/7	1/4	1/2	1				0.040149

from a sample of the Saaty matrices (Saaty 1990; Arulbalaji et al. 2019), which are shown in Table 6. In this current study, the calculated CR is 0.062017, indicating that the feature comparison was very consistent and the weights are applicable for the potential groundwater models. In order to determine potential areas of groundwater, the weighted linear combination (WLC) strategy is used.

$$BPGWI = \sum_{w=1}^m \sum_{r=1}^n (F_w \times F_r)$$

where F_w performs the normalized weight of the w thematic layer; F_r performs the relative rating of the r thematic layer; m performs the total amount of thematic layers; and n performs the total amount of subclasses in the thematic layers (Shekhar and Pandey 2015; Agarwal and Garg 2016; Kumar and Krishna 2016).

Result and discussion

Aquifer

The aquifer determines the recharge capacity as well as the storage capacity of the groundwater. The greater thickness of the aquifer represents the greater storage capacity of groundwater, and vice versa (Das and Mukhopadhyay 2018). The aquifer system of a region is considered to be a necessary parameter in describing the potentiality of groundwater in that region. This selected factor represents a wide range of geological and meteorological conditions of the given study area. It is

not easy to determine the amount of groundwater recharge in aquifers located in drought-prone semi-arid areas. There are six types of principal aquifer systems in this basin (Fig. 3). They are (a) older alluvium covering an area of 41 km² sharing 2.11%, (b) older alluvium sand and silt covering an area of 30.92 km² sharing 1.60%, (c) laterite covering an area of 555.22 km² sharing 28.71%, (d) schist (342.71 km², 17.52%), (e) Banded Gneissic Complex (903.48 km², 46.72%), and (f) basic intrusive, covering an area 60.59 km² sharing 3.13%. According to the CGWB, the annual replenishable recharge capacity of these aquifer systems is 0.89, 0.80, 0.77, 0.71, 0.63, and 0.33 (months/year), respectively. Higher annual replenishable recharge capacity values of the aquifer systems denoted higher groundwater potentiality and vice versa.

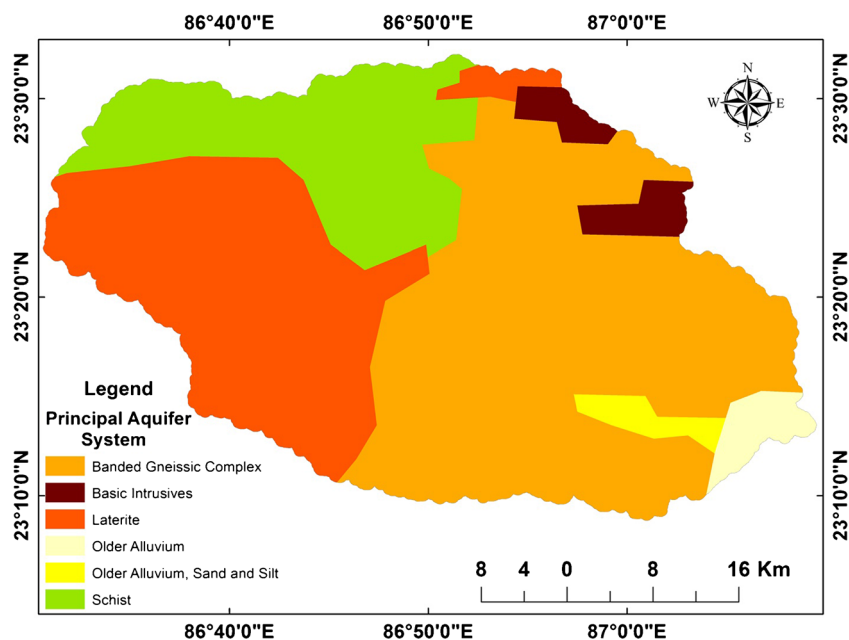
Mean annual groundwater level

Mean annual groundwater level means the yearly mean of pre-monsoon, post-monsoon, and monsoon seasons, which helps us the overall groundwater scenario of this study area. It is an important parameter which can be used to easily assess the groundwater condition of any region. The temporal and dynamic nature of groundwater level data shows the spatiotemporal difference between the monsoon and post-monsoon groundwater levels for different years (Patra et al. 2018). Here, groundwater data has been collected from the CGWB, India. Then the average ground water levels has been calculated with the help of pre-monsoon, post-monsoon (Rabi), and monsoon data. Point data is converted into thematic layer with

Table 6 Saaty’s Random consistency index (RCI) value. Source: Arulbalaji et al. (2019)

n	1	2	3	4	5	6	7	8	9	10	11	12
RI	0.0	0.0	0.58	0.90	1.12	1.24	1.32	1.41	1.45	1.49	1.51	1.48

Fig. 3 Aquifer map of the study area



the help of interpolation (IDW) method in ArcGIS environment. Shallow depth of the groundwater table is compatible for groundwater recharge and vice versa. Relation between groundwater and groundwater potentiality is highly positive which means that the area has a high potential for groundwater, and that the ground water level is nearer to the surface in this area. Here, the average depth value of the groundwater table ranges from 2.13 to 8.82 mbgl. The average underground map is classified into five categories, viz., very low (6.05–8.82 mbgl), which comprises 8.58 km² (0.44%) area, low (4.97–6.05 mbgl) comprising 240.57 km² (12.44%) area, medium (4.46–4.97 mbgl) which comprises 583.18 km² (30.15%) area, high (3.93–4.45 mbgl) which encompasses

561.96 km² (29.05%) area, and very high (2.13–3.92 mbgl) comprising 540.29 km² (27.93%) area (Fig. 4). The depth of the groundwater water table illustrates the interaction between recharge and discharge, which depends on many natural and anthropogenic activities (Arefin 2020a, b).

Lithology

Lithological property is a necessary element for determining the porosity and movement of groundwater (Jhariya et al. 2016). Permeability and porosity are the influencing factors for groundwater recharge and development (Akinlalu et al. 2017). Surface lithology is significant for soil conditions

Fig. 4 Mean annual groundwater level map of the study area

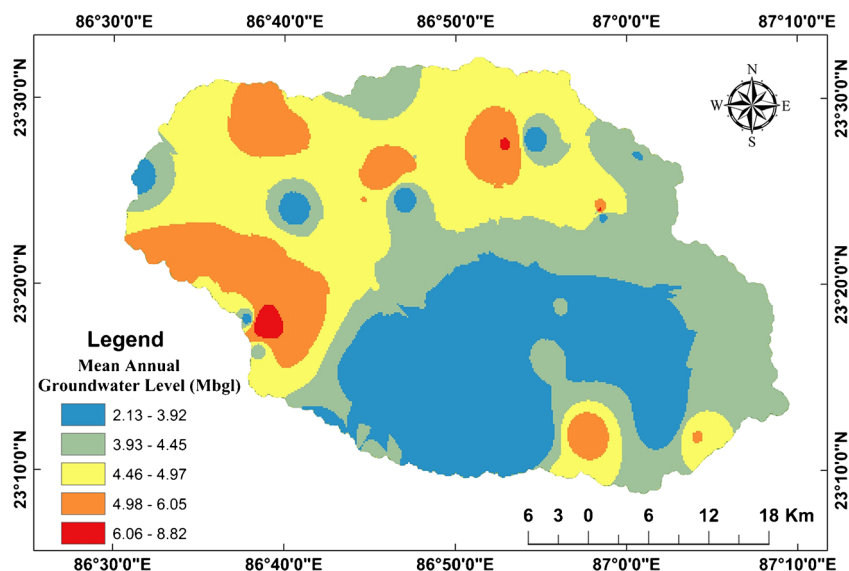
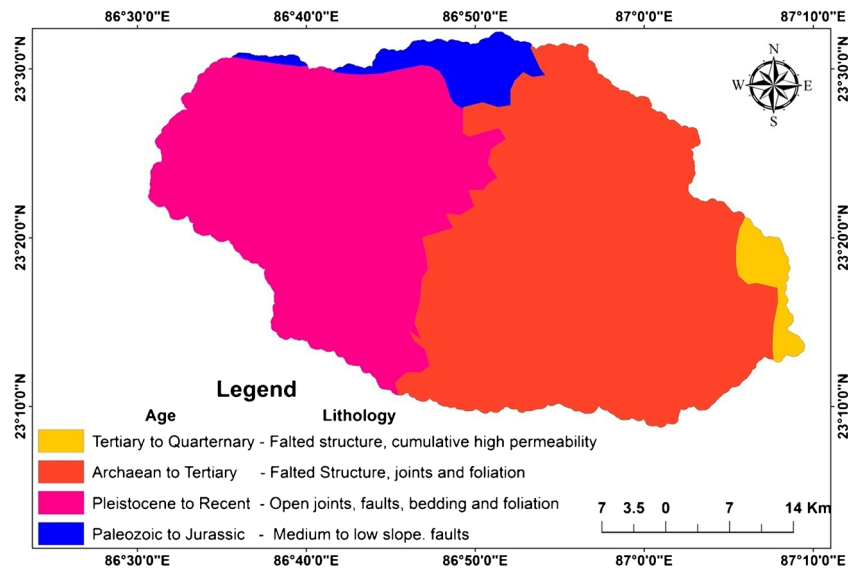


Fig. 5 Lithology map of the study area



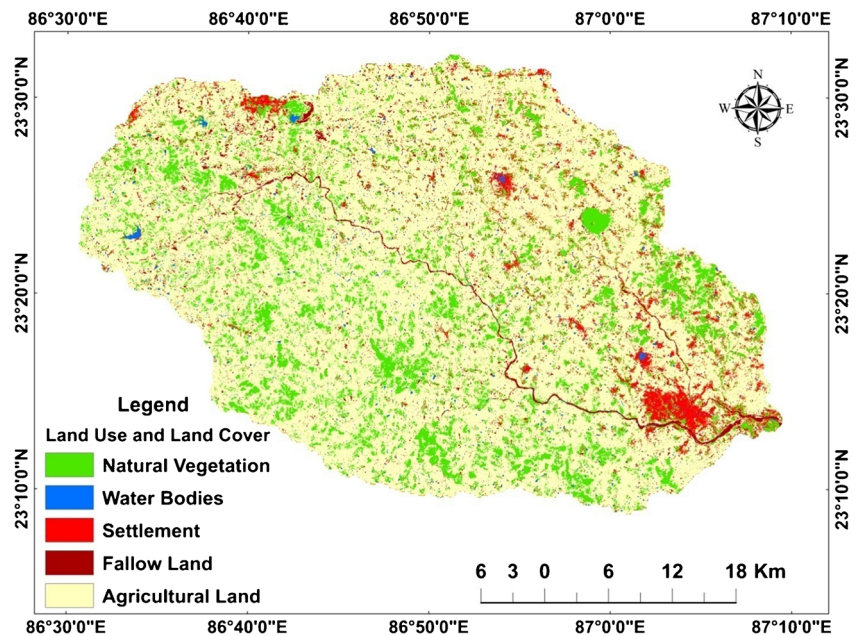
which in turn is related to the structure, adhesion, porosity, and consistency of the soil characters (Arefin 2020a, b). The geological structure of the region includes pink granite, biotite, gneiss, migmatite, mica-schist, ferruginous, gritty, sandstone, gabbro, sand, silt, and clay associated with faulted structures, joints, open joints, bedding, and foliation. The phenomenon of groundwater depends largely on the geological structure (Hachem et al. 2015). It can be seen that the field of study is usually covered by formations from four types of geological age (Fig. 5). Tertiary to Quaternary (covers 43.6338 km² area), Pleistocene to Recent (covers 772.297 km² area), Paleozoic to Jurassic (covers 85.5432 km² area), and Archaean to Tertiary (covers

1032.52 km² area). These categories covered 2.26, 39.93, 4.42, and 53.39% of the study area, respectively.

Land use and land cover

Land Use and Land Cover (LULC) affects the rate of soil moisture, surface runoff, infiltration, rate of surface runoff, groundwater, and surface water use (Ibrahim-Bathis and Ahmed 2016; Yeh et al. 2016). Five types of land use and land cover classes have been observed in study area: water body, natural vegetation, agricultural land, fallow land, and settlement (Fig. 6). The water body consists of 1.36% area, natural vegetation consists of 16.81% area,

Fig. 6 Land use and land cover map of the study area



agricultural land consists of 74.23% area, fallow land consists of 4.98%, and settlement consists of 6% area. These categories cover 26.33, 325.04, 1435.52, 50.90, and 96.25 km² of the study area, respectively. An accurate assessment of the LULC map have been measured on the basis of ground reality information verification of 126 sample points. It has been prepared by using the following matrix, which is shown in Table 7, and was calculated to 96% total accuracy with kappa coefficient (k) as 0.94889. Waterbody and the natural vegetation areas are conducive which affected the recharge of groundwater by preventing water loss through water absorption (Shaban et al. 2006; Thapa et al. 2017). Natural vegetation areas have been given moderately high weight as they gradually reduce surface flow and increase penetration rate (Bhattacharya et al. 2020). Agricultural lands also have good potentiality for groundwater recharge (Patra et al. 2018; Biswas et al. 2020). Fallow land has been assigned moderately low weight, because it rapidly reduces surface flow and penetration rates. The low probability of groundwater is allocated to the settlement areas for its low rate of infiltration, thus making settlements less important areas for groundwater recharge.

Rainfall

Rainfall is the most important input factor for groundwater recharge and an essential component of the hydrological cycle (Das and Mukhopadhyay 2018). Spatiotemporal distribution of rainfall amount, duration, and intensity are largely influenced by hydrogeological conditions ((Patra et al. 2018). The rainfall duration and intensity are affected by the penetration rate (Arefin 2020a, b). Short duration intense precipitation affects high surface runoff and low penetration, long-term low-precipitation affects higher penetration than runoff. Total average annual rainfall also influences the groundwater recharge. Higher rainfall indicates a higher probability of groundwater and lower rainfall denotes the lower probability of groundwater (Patra et al. 2018; Kadam et al. 2020; Biswas et al. 2020). The rainfall distribution map for the year 2017

was prepared using the average rainfall data collected from the IMD and with the help of ArcGIS 10.3, using the IDW interpolation method. The rain gauge stations are situated at Bankura, Central Water Commission (CWC), Kadamdeli, Phulberia, and Kashipur. Rainfall of the study area mainly depends on south-western monsoon and 80% rainfall occurred between June and September months. Based on the distribution of average annual rainfall, the entire study area has been divided into five sections, viz., very low (1398–1453 mm), low (1454–1498 mm), medium (1499–1539 mm), high (1540–1539 mm), and very high (1585–1631 mm), which cover about 282 km² (15%), 390 km² (20%), 538 km² (28%), 385 km² (20%), and 339 km² (17%) areas, respectively. The amount of average rainfall is higher in the eastern part than the western part (Fig. 7).

Drainage density

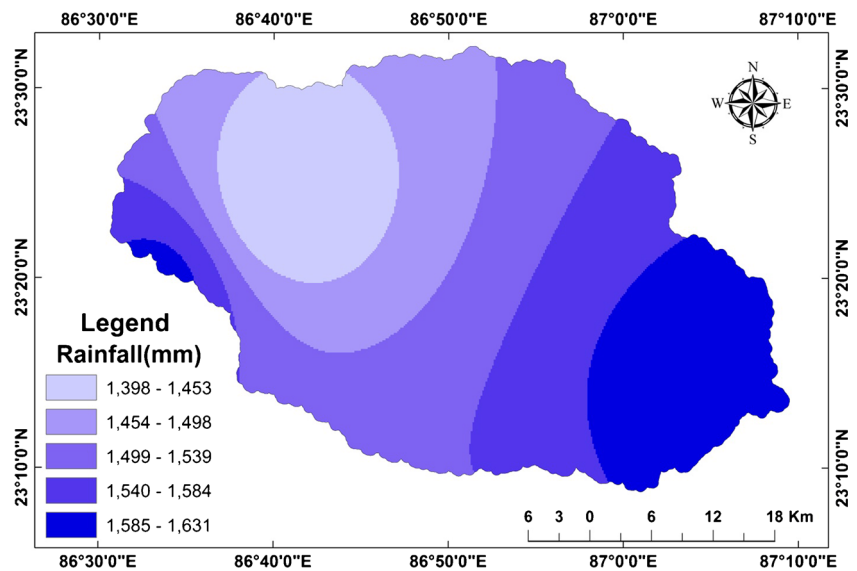
Drainage density is the total length of streams per unit area in the watershed region, and it indicates the proximity of the channel spacing (Das and Mukhopadhyay 2018; Nithya et al. 2019). Drainage density relies on the degree of fluvial isolation and is influenced by a number of factors including resistance to erosion, the structure of rocks (lithology), penetration capacity, plant cover, surface roughness, and runoff intensity indicators, and higher levels of climatic conditions (Kanagaraj et al. 2018; Patra et al. 2018; Arefin 2020a, b). Areas with high drainage density will have restricted penetration, exacerbate sufficient runoff, and vice versa. Thus, lower density values are more helpful for higher groundwater recharge and higher weights are imposed (Das and Mukhopadhyay 2018; Patra et al. 2018; Nithya et al. 2019; Arulbalaji et al. 2019; Biswas et al. 2020; Arefin 2020a, b). According to drainage density, the field of study is divided into five subclasses, namely “very good” (2–3.6 km/km²), “good” (1.5–1.9 km/km²), “medium” (1.2–1.4 km/km²), “poor” (0.73–1.1 km/km²), and “very poor” (0.0021–0.72 km/km²) covering an area of 105.677, 356.796, 540.264, 603.442, and 327.831 km² accounting for 5.46, 18.45, 27.94, 31.20, and 16.95%, respectively, of the total area (Fig. 8).

Table 7 Land use and land cover matrix

	Natural vegetation	Water bodies	Settlement	Fallow land	Agricultural land	Total (user)	Users accuracy	Producer accuracy
Natural vegetation	33	0	0	0	0	33	100	100
Water bodies	0	16	0	0	0	16	100	100
Settlement	0	0	19	1	0	20	95	100
Fallow land	0	0	0	17	2	19	89.47368	85
Agricultural land	0	0	0	2	36	38	94.73684	94.73684
Total (producer)	33	16	19	20	38	126		

Overall accuracy= 96.03175; Kappa coefficient = 94.88927

Fig. 7 Rainfall map of the study area



Soil drainage

Soil drainage is a physical component of the global hydroelectric cycle. This natural process provides water that supports soil moisture, springs, seeps, stream base flow, aquifer recharge, and recharge of some effluent streams (Fausey 2005; Tabor et al. 2017). The combinations of soil drainage concepts with other soil properties, for example, soil moisture, depth to bedrock, texture, and organic-matter content, affect long-term wetness which directly affects the recharge of groundwater. Here the relation between soil drainage and groundwater is directly proportional to the infiltration. A high soil drainage area increases the high infiltration rate and vice versa. So, usually, the depth of the water table is related to soil drainage class concept. That is shown in Table 8. The field of study is basically covered by ten classes (Fig. 9), and the map was further reclassified into seven groups: excessively drained (172.951

km², 65.31%), somewhat excessively drained (718.65 km², 37.20%), well-drained (321.27 km², 16.63%), mod. well-drained (52.93 km², 2.74%), imperfectly well-drained (399.03 km², 20.65%), imperfectly moderately drained (124.10 km², 6.42%), and imperfect drained (143.15 km², 7.41%).

Soil texture

Soil texture is an essential factor for assessing the physical condition of soil and is directly related to soil porosity, adhesion, and consistency (Patra et al. 2018). The penetration and permeability of water depends on the soil texture, and therefore, the soil texture affects the percolation rate and groundwater recharge (Kumar and Krishna 2016; Das and Mukhopadhyay 2018; Patra et al. 2018). The finer soil texture indicates the low infiltration capacity and as a result, the less groundwater will be recharged and vice versa (Doll and

Fig. 8 Drainage density map of the study area

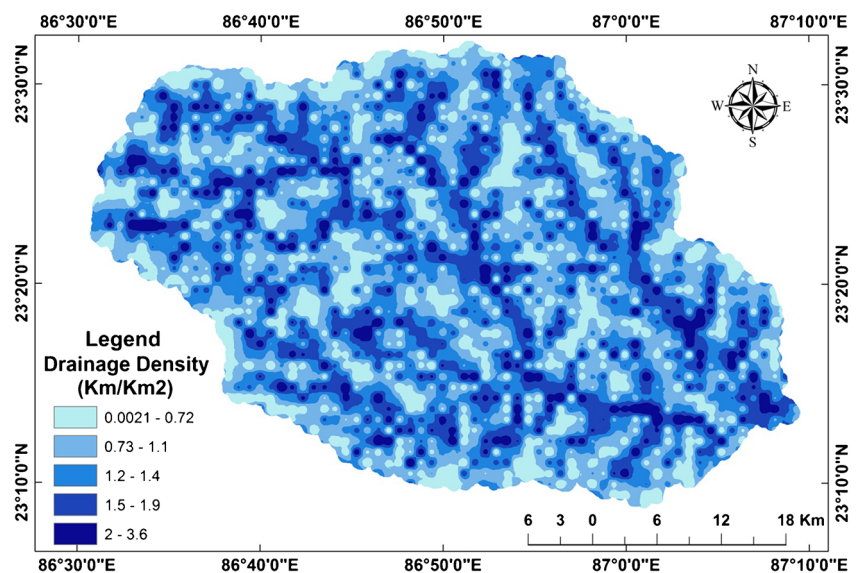


Table 8 Generalized relations between soil drainage classes and depth of water table. Source—Schaeztl (2013)

Soil drainage class	Excessively drained	Somewhat excessively drained	Well-drained	Mod. well-drained	Imperfectly well-drained	Imperfectly mod drained	Imperfectly drained
Typical depth to water table (cm)	> 150	> 150	100–150	75–125	30–75	< 30–50	0–15

Fiedler 2008). Sandy soil textures have a higher infiltration rate and a lower runoff potential. therefore, it is given a higher weight. The texture of the clay with the lowest infiltration rate and the highest runoff potential is given less priority (Kumar and Krishna 2016). Here, sandy mixed soil texture has been given relatively higher weights. The loamy soil texture was given medium priority because it consolidates sand, silt, and clay particles so that soils have a moderate penetration rate, while the gravelly texture with moderately low infiltration rate then has been given moderately lower priority after the clayey soil texture. Based on soil texture data, the study area is divided into eighteen types of soil texture classes (Fig. 10), and then, the thematic data has been reclassified into five soil texture groups, namely clay groups, gravelly groups, loamy groups, sandy-clay groups, and sandy-loam groups. These categories cover 420.19 km² (21.76%), 246.65 km² (12.75%), 528.67 km² (27.34%), 285.103 km² (14.74%), and 453.34 km² (23.44 %) of the study area, respectively.

NDVI

NDVI (normalized difference vegetation index) is a remote sensing–based vegetation index that can monitor vegetation condition. NDVI means the normal difference between the red and near-infrared bands from an image. The NDVI range varies from – 1 to + 1. NDVI value of (– 1 to 0) zero or less

indicates snow, water, sand, and cloud. The value 0 to 0.1 indicates bear rock, barren land, or built-up area, 0.1 to 0.2 value indicates shrub and grassland, 0.2 to 0.4 value shows sparse vegetation or senescing crops, 0.4 to 0.8 denotes dense vegetation, and 0.8 to 1 indicates very healthy dense vegetation (Akbar et al. 2019; Parmar et al. 2019). The healthy and dense vegetation in an area often seems to be associated with good groundwater recharge. Therefore, the higher the value, the more weight is assigned, and sparse vegetation, shrub, and grassland are assigned moderated weight, but the value (0 to – 1) showing waterbodies has been assigned high weight (Patra et al. 2018). The NDVI map of the study area has been classified into the following five zones: very low (– 0.134 to 0), low (0.001 to 0.1), moderate (0.101 to 0.2), high (0.201 to 0.387) (Fig. 11). These categories covered 7.97 km² (0.41%), 135.16 km² (6.99%), 1634.25 km² (84.50%), and 156.63 km² (8.10%) of area respectively.

Elevation

The elevation map of the field of study directly reflects the roughness of the terrain. Elevation is directly proportional to the runoff rate and inversely proportional to infiltration. That means high elevation areas will have limited penetration and rapid runoff. Thus, the lower elevation is more suitable for higher groundwater availability (Godebo 2005; Patra et al.

Fig. 9 Soil drainage map of the study area

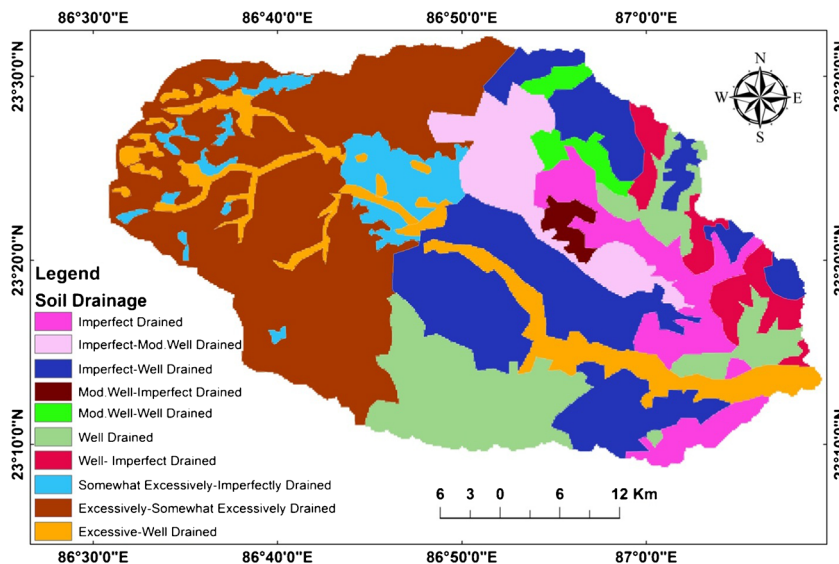
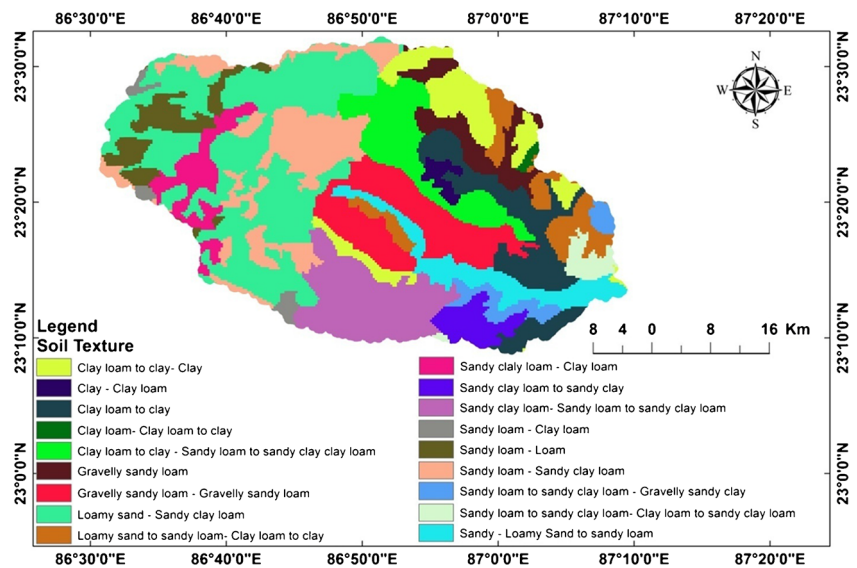


Fig. 10 Soil texture map of the study area



2018). The regions having a higher elevation (dissected plateau region) has a higher probability of high flow rate, and decreased rate of infiltration. Therefore, this class has been assigned low weight. And a low elevation flat region with a limited runoff rate retains water by inducing further infiltration of water recharge, so this class has been assigned high weight. The weight of the rest of the classes is determined based on the relationship between runoff and penetration rate. The study area is divided into five classes, which are as follows: terrain height (Fig. 12), very low (69–112 m), low (113–140 m), moderate (141–168 m), high (169–201 m), and very high (202–255 m). These classes have covered 318.379 km² area (16.46%), 538.565 km² area (27.85%), 537.069 km² area

(27.75%), 376.264 km² area (19.46%), and 163.734 km² area (8.47%), respectively. Generally, the three main natural divisions of this terrain are the undulating plateau region, the uplands, and the plains. In this area, some separately dissected monadnocks are located. The elevation of the study area decreases towards the west to east.

Curvature

Curvature is a vital quantitative interpretation of the character of the earth’s surface (Nair et al. 2017). The curvature values represent the morphometrics of the topography of any region and it may be concave, flat, or convex (Arulbalaji et al. 2019).

Fig. 11 NDVI map of the study area

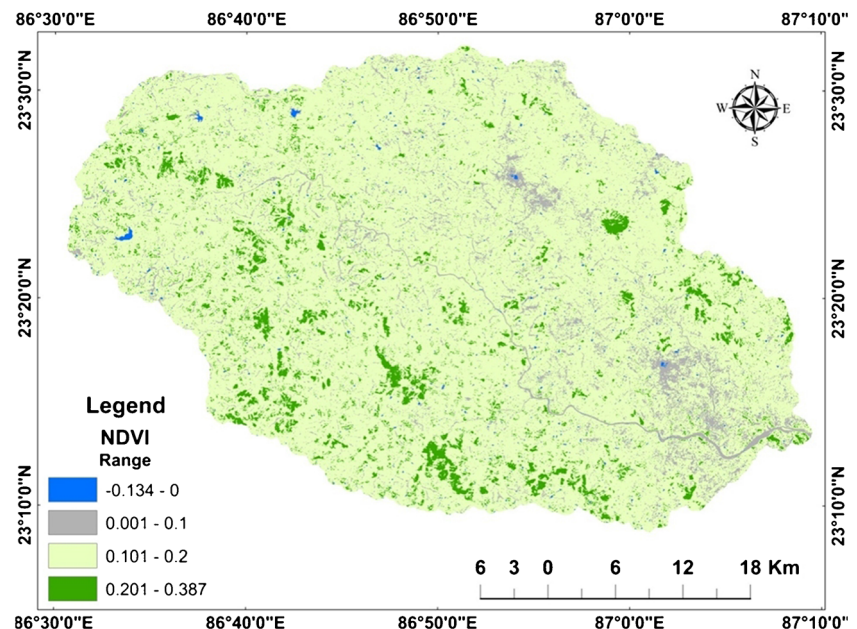
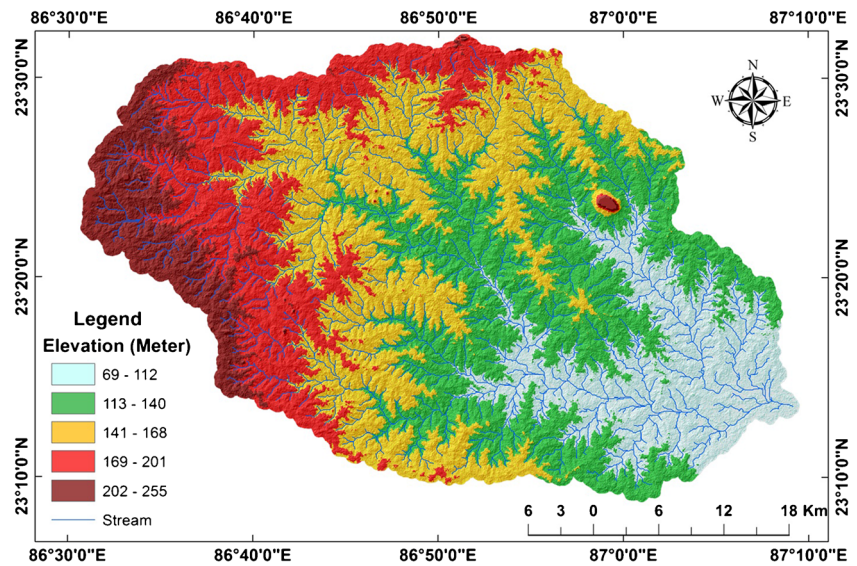


Fig. 12 Elevation map of the study area



The convex part has more runoff and less infiltration resulting in less groundwater recharge. The opposite is true for the concave regions (Nair et al. 2017; Biswas et al. 2020). When curvature value is positive, it indicates the surface is convex. Zero value indicates plain surface and a negative value indicates a surface that is concave (Biswas et al. 2020). Here the convex surface has been given less weight, the flat surface is given medium weight, and the concave surface is given more weight depending on their topographic condition and infiltration rate. The field of study is basically covered by three categories, namely: convex (0.001 to 7), flat (− 0.000899 to 0), and concave (− 3.67 to − 0.0009). Most of the study area falls under the concave area which is 798 km² (41.26%). Total 729-km² (37.69%) and 407 km² (21.05%) of the study area is covered with convex and flat area, respectively (Fig. 13).

Slope

Slope is another significant topographical indicator for determining the potential zone of groundwater. Slope indirectly controls the penetration of surface water into aquifer and influences the development of drainage patterns of a river basin (Nithya et al. 2019). It controls the rate of surface runoff and also infiltration of water. Slope is directly proportional to runoff rate and inversely proportional to infiltration (Das and Mukhopadhyay 2018; Biswas et al. 2020). Areas with high slopes have been given less weight and areas with low slopes have been given comparatively lesser weight based on their runoff and infiltration rates. The slope map of the study area has been categorized into the following five classes, namely: very steep slope (> 7) covering

Fig. 13 Curvature map of the study area

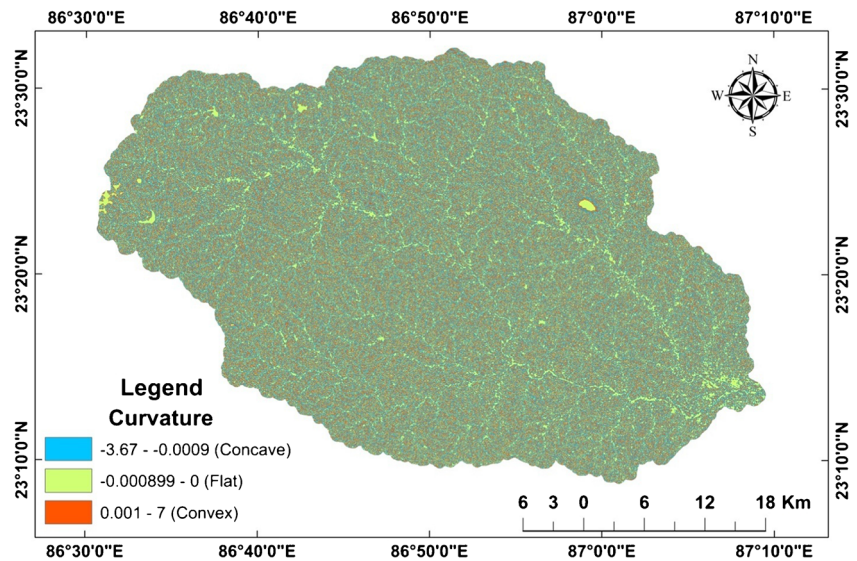
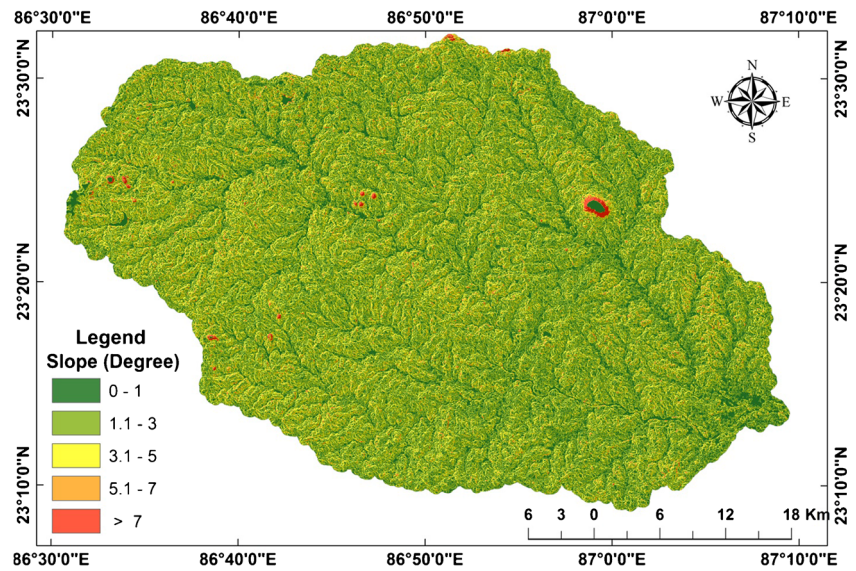


Fig. 14 Slope map of the study area



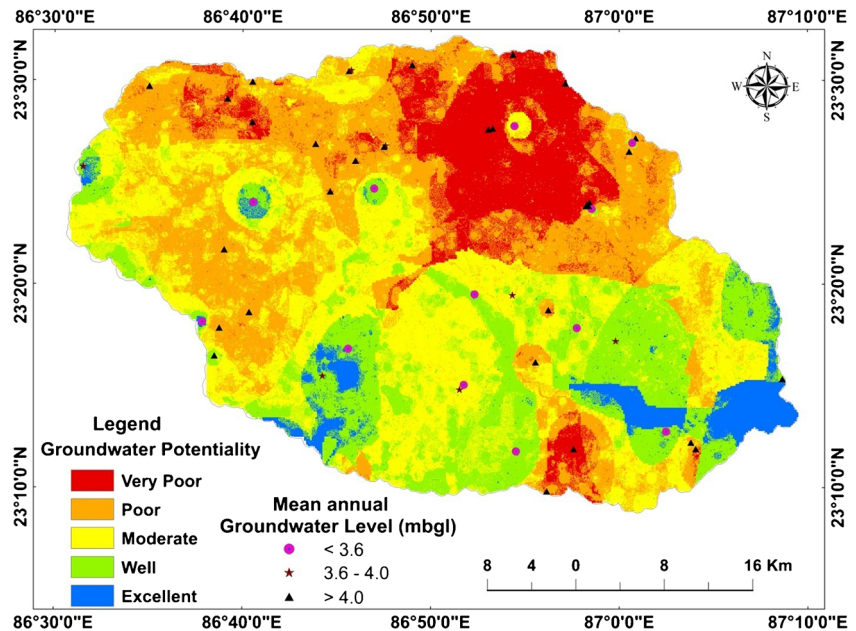
9.96 km² (0.51%), steep slope (5–7) covering 59.44 km² (3.07%), moderate slope (3–5) covering 410.31 km² (21.22%), gentle slope (1–3) covering 1077.38 km² (55.71%), and flat slope (0–1) covering 376.90 km² (19.49%) area (Fig. 14).

Groundwater potentiality zone

The main geo-environmental factors which have probable influence on groundwater potentiality in this region are aquifer media, average groundwater level, lithology, land use and land cover (LULC), rainfall, drainage density, soil drainage, soil texture, NDVI, elevation, curvature, and slope. Groundwater potentiality zone mapping has been delineated

for the study area based on multi-influencing AHP technique and GIS-weighted overlay analysis by using the ArcGIS 10.3 platform. On the basis output map, the field of study revealed five distinctly classified zones, namely: very poor, poor, moderate, well, and excellent, covering an area of 256.87, 581.79, 607.91, 381.58, and 91.36 km², respectively. About 13.38% of the calculated field groundwater has a very poor probability, 30.30% has a poor probability, 31.66% has moderate probability, 19.87% has a well probability, and 4.76% has an excellent probability (Fig. 15). The results demonstrate that a well and excellent GWPZ are concentrated in the southeastern and southern part of the basin particularly in Bankura-I, Bankura-II, Onda, and Pancha regions, due to the availability of sandy textured, excessively well-drained soil, high intensity

Fig. 15 Groundwater potentiality zone map of Dwarakeshwar River basin



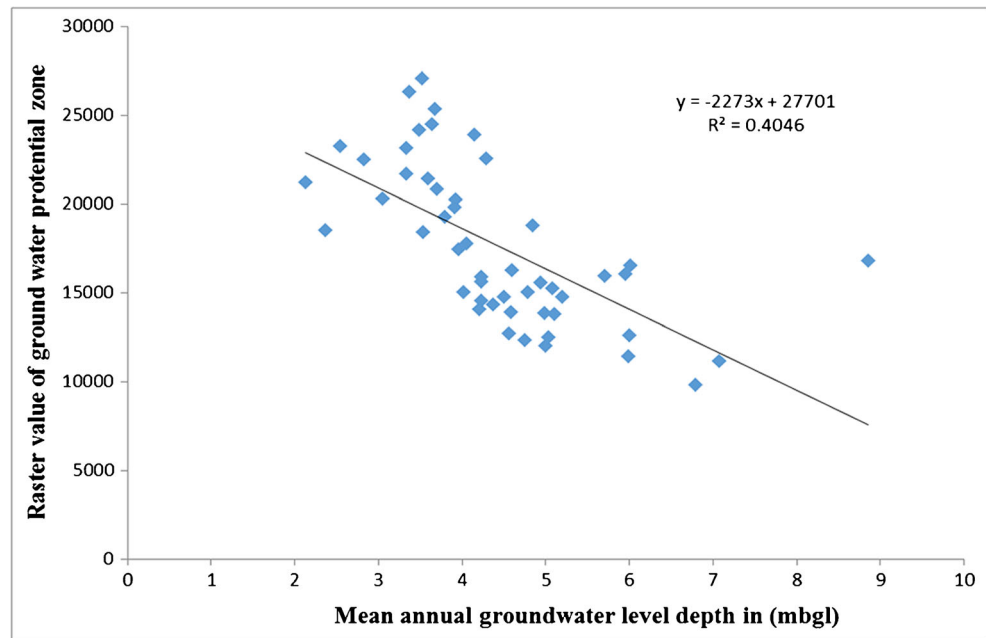
of rainfall, agricultural land, and gentle slope, with an excellent infiltration capability. On the other hand, the presence of Paleozoic to Jurassic formations, clayey texture, imperfect and imperfectly moderately drained soils, very low NDVI, high elevation, basic intrusives, and Banded Gneissic Complex as aquifer media in the northern and northwestern regions of the study area have less primary significance, with very little effect on groundwater availability. That is why the areas represent very poor to poor groundwater potentiality. With only a

few parts to the southwest of the study area, there is a moderate presence of secondary porosity with moderate amount of rainfall, somewhat excessively well-drained soil and vegetation in the location, allowed for the availability of moderate amounts of groundwater. A geospatial assessment of the potential map of groundwater shows that the upper portion of the upper Dwarakeshwar River basin is moderately poor, the upper-middle portion is very poor, lower-middle portion is moderately well, and the lower portion is good.

Table 9 Dug well locations and accuracy assessment through the check of mean annual groundwater level depth using binary coding

Block	Site	Latitude	Longitude	Mean annual groundwater level	Raster value	Reclass value	Binary code
Hura	Jhapra	23.4295	86.5254	3.676667	25,371	5	0
Para	Anara	23.4952	86.5839	4.846667	18,779	3	0
Kashipur	Naduara	23.4987	86.6753	4.783333	15,043	2	1
Kashipur	Rangani	23.4852	86.6532	6	12,588	1	1
Kashipur	Palashkhoa	23.4659	86.6753	5.103333	13,783	1	1
Kashipur	Napara	23.4002	86.676	3.37	26,297	5	1
Kashipur	simla2	23.3617	86.6503	5.083333	15,227	2	1
Hura	Katagora	23.3103	86.6724	5.7	15,919	2	1
Hura	Lalpur2	23.3024	86.631	3.52	27,077	5	1
Hura	Hura	23.2974	86.646	8.86	16,804	2	1
Hura	Raheradhi	23.2746	86.6418	4.14	23,892	4	0
Hura	Bishpuria	23.2582	86.7374	3.636667	24,496	4	0
Hura	Jorberia	23.2803	86.7602	3.49	24,189	4	1
Kashipur	Kapasitha	23.409	86.7441	4.98	13,832	1	1
Kashipur	indrabil24	23.4481	86.7312	4.936667	15,566	2	1
Kashipur	Gaurandih B	23.4343	86.7664	5.95	16,042	2	1
Kashipur	Indrabil	23.4114	86.7831	3.33	23,142	4	1
Raghunathpur1	Bero-1	23.5076	86.7607	4.056667	17,748	3	1
Raghunathpur1	Bero-2	23.5084	86.7627	3.96	17,460	3	1
Kashipur	Gaurandih B	23.4468	86.7932	3.92	20,274	3	1
Kashipur	Gaurandih1	23.4457	86.7917	6.01	16,514	2	1
Santuri	Leadson	23.5125	86.8167	4.5	14,753	2	1
Saltora	Murulu	23.5211	86.9059	4.56	12,725	1	1
Saltora	Kashtora 1	23.4975	86.9523	4.753333	12,331	1	1
Saltora	Lakhanpur	23.4528	87.0145	4.23	15,866	2	1
Saltora	Lakhanpur A	23.449	87.0116	3.59	21,406	4	0
Saltora	Lakhanpur2	23.4418	87.0087	4.223333	14,545	2	1
Chatna	Dhaban	23.4628	86.9073	3.046667	20,289	3	0
Chatna	susunia-2	23.4608	86.888	5	11,995	1	1
Chatna	susunia-1	23.4599	86.8841	6.793333	9813	1	1
Chatna	susunia2	23.3999	86.9736	7.073333	11,174	1	1
Chatna	Lakhanpur1	23.3948	86.9756	2.36	18,542	3	0
Chatna	Susunia2	23.3974	86.9728	5.026667	12,501	1	1
Chatna	Majia-2	23.3984	86.9713	4.233333	15,620	2	1
Chatna	Majia	23.3971	86.9707	4.366667	14,352	2	1
Bankura-2	Makurgram1	23.2555	87.1443	4.283333	22,582	4	0
Indpur	Indpur	23.1636	86.9359	4.583333	13,919	1	1
Chatna	Kenjakura	23.2469	86.8588	3.79	19,263	3	1
Chatna	Kenjakura A	23.2507	86.8626	3.533333	18,435	3	0
Indpur	Shalboni-2	23.1965	86.9087	2.83	22,492	4	0
Indpur	Bhagabanpur1	23.1984	86.9596	5.986667	11,430	1	1
Onda	Bankura	23.2127	87.0415	2.543333	23,276	4	0
Onda	Jagadalla	23.2036	87.0634	4.596667	16,275	2	1
Onda	Gorabari	23.1984	87.0677	5.193333	14,772	2	1
Bankura-I	Gouripur	23.2869	86.9968	3.696667	20,851	4	0
Chatna	Kenjakura 1	23.2693	86.9259	4.2	14,053	2	1
Chatna	Chhatna	23.2974	86.9625	2.126667	21,213	4	0
Chatna	Kamalpore	23.3121	86.9373	4.013333	15,015	2	1
Chatna	Chaintore	23.3245	86.9054	3.91	19,819	3	1
Chatna	Budhanpur	23.325	86.8721	3.333333	21,724	4	1

Fig. 16 Relationship between the groundwater potential zone and mean annual groundwater level



Validation

Validation is an important part of any research, and without a validation part, the whole research becomes impractical. To validate the classified groundwater potential zones, groundwater level data of 50 dug wells were collected from the Central Ground Water Board (CGWB). Dug well locations and mean annual groundwater level depth data are shown in

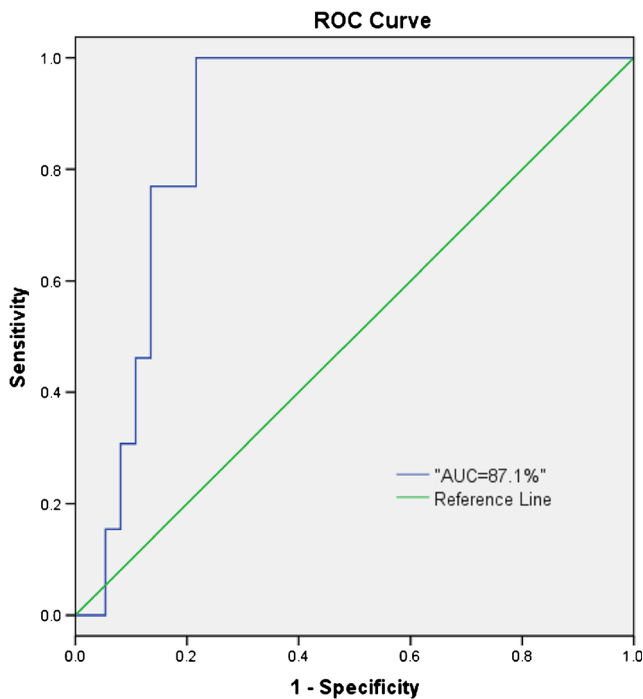


Fig. 17 ROC curve for the groundwater potential zone map of upper Dwarakeshwar River basin

the map of the study area (Fig. 1 and Table 9). On the basis of mean annual groundwater level ranges of the study area, the area has been grouped into four categories, viz. > 4.2 mbgl as low, 3.6–4.2 mbgl as moderate, 3–3.6 mbgl as well, and < 3 mbgl as excellent. Then, the raster value of GWPZ was reclassified and matched with the mean annual groundwater level. It has been noted that there is a strong negative correlation between the groundwater potential zone and mean annual groundwater level depth. Hence, regions having greater depth in water level have low-groundwater potential and regions having less depth show a high groundwater potential (Fig. 16). It is seen for a match, which matches and which does not match with binary code. The value 1 represents that the condition agreed and 0 represents the condition is disagreed. This validation was accomplished by the receiver operating characteristic (ROC) curve, because the receiver operating characteristic curve is a widely used technique to validate GWPZ (Naghibi and Pourghasemi 2015; Zabihi et al. 2016; Guru et al. 2017; Das and Mukhopadhyay 2018). Based on the relationship between AUC values and forecast accuracy, the AUC values can be divided into the following categories: “0.9–1.0” excellent, “0.8–0.9” very good, “0.7–0.8” good, “0.6–0.7” average, and “0.5–0.6” poor (Naghibi and Pourghasemi 2015; Rahmati et al. 2016, Guru et al. 2017; Arabameri et al. 2018; Senapati and Das 2020). The AUC values range from 0.5 to 1.0. A value near 1.0 indicates the highest degree of accuracy, and a value near 0.5 indicates ambiguity in the model. In the recent study, prediction rates were also measured using the analyze tool of SPSS software under the ROC curve method (Fig. 17). It was found that the area under curve value (AUC) is 0.871. The results of AUC (0.871) and std. error (0.050) under non-parametric estimates

indicate that it is a well-predicted model with an accuracy of 87.1%. Finally, the groundwater potential zones showed that the model gives very good results in the present research.

Conclusions

In this study, the AHP technique including remote sensing and GIS has been applied to delineate groundwater potential areas in the upper Dwarakeshwar River basin, West Bengal. A map of the groundwater potentiality zone has been prepared by combining the thematic levels from a total of 12 geo-environmental parameters related to groundwater, which are as follows: aquifer media, average groundwater, lithology, land use and land cover, rainfall, drainage density, soil drainage, soil texture, NDVI, elevation, curvature, and slope. The results have been validated with the mean annual groundwater level data (ranging from 8.86 to 2.13 m bgl) of 50 dug wells through the ROC curve. The integrated map of the study area has been classified into five groundwater potential zones, viz. very poor, poor, moderate, well, and excellent, covering an area with 13.38%, 30.30%, 31.66%, 19.87%, and 4.76%, respectively. It is also observed from the output results that the good (well and excellent) groundwater potential area is located only in the extended alluvial plain and peneplain section of the study area with favorable hydrogeomorphologic conditions like suitable aquifer media (older alluvium, sand, silt, and laterite) low elevation, low slope, sandy textured, excessively well-drained soil, land use and land cover (agricultural and natural vegetation), and optimum rainfall. However, low-groundwater probability areas are the ones where geo-environmental elements increase the runoff and greatly reduce the rate of infiltration. All of these areas are considered a zone for artificial groundwater recharge processes. These areas can be chosen to store rainwater for recharge structure constructions like structural dams, check dams, water absorption trenches, horizontal dykes, rock-filled earthwork, and farm ponds, and to capture excess surface runoff. Thus, the importance of the current systematic study is the methodology adopted, based on reasonable conditions, which can be also applied with similarly smaller and appropriate changes in India or abroad. It is very helpful for planning sustainable management systems for groundwater, land use, and water resource management in regions. The advantage of this method is that it is a low-cost, effective method which reduces the time consumed for doing the required work, with less labor, compared to the conventional methods of study. To fulfill the urgent need of improving groundwater management practices in an era of resource depletion, potential groundwater maps can be created using this method.

Acknowledgements This work was carried under the Junior Research Fellowship (JRF) scheme, University Grant Commission (UGC), New Delhi. The authors are very grateful to Geological Survey of India (GSI), Indian Meteorological Department (IMD), United States Geological Survey (USGS), Central Groundwater Board (CGWB), and National Bureau of Soil Survey and Land Use planning (NBSS & LUP) for providing the necessary data.

Declarations

Conflict of interest The authors declare no competing interests.

References

- Agarwal R, Garg PK (2016) Remote sensing and GIS based groundwater potential and recharge zones mapping using multi-criteria decision making technique. *Water Resour Manag* 30(1):243–260. <https://doi.org/10.1007/s11269-015-1159-8>
- Ahmed JB II, Mansor S (2018) Overview of the application of geospatial technology to groundwater potential mapping in Nigeria. *Arab J Geosci* 11(17):504. <https://doi.org/10.1007/s12517-018-3852-4>
- Akbar TA, Hassan QK, Ishaq S, Batool M, Butt HJ, Jabbar H (2019) Investigative spatial distribution and modelling of existing and future urban land changes and its impact on urbanization and economy. *Remote Sens* 11(2):105. <https://doi.org/10.3390/rs11020105>
- Akinlalu AA, Adegbuyiro A, Adiat KAN, Akeredolu BE, Lateef WY (2017) Application of multi-criteria decision analysis in prediction of groundwater resources potential: a case of Oke-Ana, Ilesa area Southwestern, Nigeria. *NRIAGJ Astron Geophys* 6:184–200. <https://doi.org/10.1016/j.nrjag.2017.03.001>
- Al-Abadi AM (2015) Groundwater potential mapping at northeastern Wasit and Missan governorates, Iraq using a data-driven weights of evidence technique in framework of GIS. *Environ Earth Sci* 74: 1109–1124. <https://doi.org/10.1007/s12665-015-4097-0>
- Arabameri A, Pradhan B, Pourghasemi HR, Rezaei K (2018) Identification of erosion-prone areas using different multi-criteria decision-making techniques and GIS. *Geomatics, Nat Hazards Risk* 9(1):1129–1155. <https://doi.org/10.1080/19475705.2018.1513084>
- Arefin R (2020a) Groundwater potential zone identification using an analytic hierarchy process in Dhaka City, Bangladesh. *Environ Earth Sci* 79(11). <https://doi.org/10.1007/s12665-020-09024-0>
- Arefin R (2020b) GIS and remote sensing based weighted linear combination (WLC) of thematic layers for groundwater potentiality study at Plio-Pleistocene elevated tract in Bangladesh. *Groundw Sustain Dev* 10:100340. <https://doi.org/10.1016/j.gsd.2020.100340>
- Arulbalaji P, Padmalal D, Sreelash K (2019) GIS and AHP techniques based delineation of groundwater potential zones: a case study from southern Western Ghats, India. *Sci Rep* 9(1):1–17. <https://doi.org/10.1038/s41598-019-38567-x>
- Bera A, Das S (2021) Water resources management in semi-arid Purulia District of West Bengal, in the context of sustainable development goals. In *Groundwater and Society*. <https://doi.org/10.1007/978-3-030-64136-8>
- Bera A, Mukhopadhyay BP, Das D (2019) Landslide hazard zonation mapping using multi-criteria analysis with the help of GIS techniques: a case study from Eastern Himalayas, Namchi, South Sikkim. *Nat Hazards* 96(2):935–959. <https://doi.org/10.1007/s11069-019-03580-w>
- Bera A, Mukhopadhyay BP, Barua S (2020) Delineation of groundwater potential zones in Karha river basin, Maharashtra, India, using AHP and geospatial techniques. *Arab J Geosci* 13(15):1–21. <https://doi.org/10.1007/s12517-020-05702-2>

- Bera A, Mukhopadhyay BP, Biswas S (2021) Aquifer vulnerability assessment of Chaka river basin, Purulia, India using GIS-based DRASTIC model. In Geostatistics and geospatial technologies for groundwater resources in India. Springer International Publishing, pp. 1–21.
- Bhattacharya S, Das S, Das S, Kalashetty M, Warghat SR (2020) An integrated approach for mapping groundwater potential applying geospatial and MIF techniques in the semiarid region. *Environ Dev Sustain* <https://doi.org/10.1007/s10668-020-00593-5>
- Bhunia GS, Samanta S, Pal DK, Pal B (2012) Assessment of groundwater potential zone in Paschim Medinipur District, West Bengal—a mesoscale study using GIS and remote sensing approach. *J Environ Earth Sci* 2(5):41–59
- Bhunia P, Das P, Maiti R (2020) Meteorological drought study through SPI in three drought-prone districts of West Bengal, India. *Earth Syst Environ* 4(1):43–55. <https://doi.org/10.1007/s41748-019-00137-6>
- Biswas S, Mukhopadhyay BP, Bera A (2020) Delineating groundwater potential zones of agriculture dominated landscapes using GIS based AHP techniques: a case study from Uttar Dinajpur district, West Bengal. *Environ Earth Sci* 79(12):1–25. <https://doi.org/10.1007/s12665-020-09053-9>
- Calow RC, Robins NS, MacDonald AM, MacDonald DM, Gibbs BR, Orpen WR, Mtembezeka P, Andrews AJ, Appiah SO (1997) Groundwater management in drought-prone areas of Africa. *Int J Water Resour Dev* 13(2):241–262. <https://doi.org/10.1080/07900629749863>
- Chowdhury A, Jha MK, Chowdhury VM, Mal BC (2009) Integrated remote sensing and GIS-based approach for assessing groundwater potential in West Medinipur district, West Bengal, India. *Int J Remote Sens* 30(1):231–250. <https://doi.org/10.1080/01431160802270131>
- Das N, Mukhopadhyay S (2018) Application of multi-criteria decision making technique for the assessment of groundwater potential zones: a study on Birbhumi district, West Bengal, India. *Environment, Environ Dev Sustain* 22:1–25. <https://doi.org/10.1007/s10668-018-0227-7>
- Das S, Pardeshi SD (2018) Integration of different influencing factors in GIS to delineate groundwater potential areas using IF and FR techniques: a study of Pravara basin, Maharashtra, India. *Appl Water Sci* 8(7):197. <https://doi.org/10.1007/s13201-018-0848-x>
- Das S, Choudhury MR, Nanda S (2013) Geospatial assessment of agricultural drought (a case study of Bankura District, West Bengal). *Int J Agric Sci res* 3(2):1–27
- Doll P, Fiedler K (2008) Global-scale modeling of groundwater recharge. *Hydrol Earth Syst Sci* 12:863–885. <https://doi.org/10.5194/hess-12-863-2008>
- Elmahdy SI, Mohamed MM (2015) Probabilistic frequency ratio model for groundwater potential mapping in Al Jaww plain, UAE. *Arab J Geosci* 8:2405–2416. <https://doi.org/10.1007/s12517-014-1327-9>
- Fausey NR (2005) Drainage, surface and subsurface. *Encyclopedia of Soils in the Environment*, pp 409–413. <https://doi.org/10.1016/b0-12-348530-4/00352-0>
- Ferozu RM, Jahan CS, Arefin R, Mazumder QH (2018) Groundwater potentiality study in drought prone Barind Tract, NW Bangladesh using remote sensing and GIS. *Groundw Sustain Dev* 8:205–215. <https://doi.org/10.1016/j.gsd.2018.11.006>
- Ghayoumian J, Saravi MM, Feiznia S, Nouri B, Malekian A (2007) Application of GIS techniques to determine areas most suitable for artificial groundwater recharge in a coastal aquifer in southern Iran. *J Asian Earth Sci* 30(2):364–374. <https://doi.org/10.1016/j.jseas.2006.11.002>
- Ghorbani Nejad S, Falah F, Daneshfar M, Haghizadeh A, Rahmati O (2017) Delineation of groundwater potential zones using remote sensing and GIS-based data-driven models. *Geocarto Int* 32(2):167–187. <https://doi.org/10.1080/10106049.2015.1132481>
- Ghosh PK, Jana NC (2017) Groundwater potentiality of the Kumari River Basin in drought-prone Purulia upland, Eastern India: a combined approach using quantitative geomorphology and GIS. *Sustain Water Resour Manag* 4(3):583–599. <https://doi.org/10.1007/s40899-017-0142-3>
- Gleick PH (1993) Water and conflict: fresh water resources and international security. *Int Secur* 18(1):79–112. <https://doi.org/10.2307/2539033>
- Godebo TR (2005) Application of remote sensing and GIS for geological investigation and groundwater potential zone identification, Southeastern Ethiopian Plateau, Bale Mountains and the surrounding areas. Addis A Baba University.
- Guru B, Seshan K, Bera S (2017) Frequency ratio model for groundwater potential mapping and its sustainable management in cold desert, India. *J King Saud Univ Sci* 29(3):333–347. <https://doi.org/10.1016/j.jksus.2016.08.003>
- Hachem AM, Ali E, Abdelhadi EO, Abdellahk EH, Said K (2015) Using remote sensing and GIS—multicriteria decision analysis for groundwater potential mapping in the Middle Atlas Plateau, Morocco. *Res J Recent Sci* 4(7):33–41
- Hellegers P, Zilberman D, van Ierland E (2001) Dynamics of agricultural groundwater extraction. *Ecol Econ* 37(2):303–311. [https://doi.org/10.1016/s0921-8009\(00\)0288-3](https://doi.org/10.1016/s0921-8009(00)0288-3)
- Horiáková N, Jurík L, Hrablík CH, Cagáňová D, Babčanová D (2019) AHP method application in selection of appropriate material handling equipment in selected industrial enterprise. *Wirel Netw* 27:1683–1691. <https://doi.org/10.1007/s11276-019-02050-2>
- Ibrahim-Bathis K, Ahmed SA (2016) Geospatial technology for delineating groundwater potential zones in Doddahalla watershed of Chitradurga district, India. *Egypt J Remote Sens Space Sci* 19(2):223–234. <https://doi.org/10.1016/j.ejrs.2016.06.002>
- Jasrotia AS, Kumar R, Taloor AK, Saraf AK (2019) Artificial recharge to groundwater using geospatial and groundwater modelling techniques in North Western Himalaya, India. *Arab J Geosci* 12(24):774. <https://doi.org/10.1007/s12517-019-4855-5>
- Jha MK, Chowdhury VM, Chowdhury A (2010) Groundwater assessment in Salboni Block, West Bengal (India) using remote sensing, geographical information system and multi-criteria decision analysis techniques. *Hydrogeol J* 18(7):1713–1728. <https://doi.org/10.1007/s10040-010-0631-z>
- Jhariya DC, Kumar T, Gobinath M, Diwan P, Kishore N (2016) Assessment of groundwater potential zone using remote sensing, GIS and multi-criteria decision analysis techniques. *J Geol Soc India* 88(4):481–492. <https://doi.org/10.1007/s12594-016-0511-9>
- Kadam AK, Umrikar BN, Sankhua RN (2020) Assessment of recharge potential zones for groundwater development and management using geospatial and MCDA technologies in semiarid region of Western India. *Appl Water Sci* 2(2):312. <https://doi.org/10.1007/s42452-020-2079-7>
- Kanagaraj G, Suganthi S, Elango L, Magesh NS (2018) Assessment of groundwater potential zones in Vellore district, Tamil Nadu, India using geospatial techniques. *Earth Sci Inform* 12(2):211–223. <https://doi.org/10.1007/s12145-018-0363-5>
- Kolanuvada SR, Ponpandian KL, Sankar S (2019) Multi-criteria-based approach for optimal siting of artificial recharge structures through hydrological modeling. *Arab J Geosci* 12(6):190. <https://doi.org/10.1007/s12517-019-4351-y>
- Kumar A, Krishna AP (2016) Assessment of groundwater potential zones in coal mining impacted hard-rock terrain of India by integrating geospatial and analytic hierarchy process (AHP) approach. *Geocarto Int* 33(2):105–129. <https://doi.org/10.1080/10106049.2016.1232314>
- Kumru M, Kumru PY (2014) Analytic hierarchy process application in selecting the mode of transport for a logistics company. *J Adv Transp* 48(8):974–999. <https://doi.org/10.1002/atr.1240>

- Lee S, Lee CW (2015) Application of decision-tree model to groundwater productivity-potential mapping. *Sustainability* 7(10):13416–13432. <https://doi.org/10.3390/su71013416>
- Lee S, Song KY, Kim Y, Park I (2012) Regional groundwater productivity potential mapping using a geographic information system (GIS) based artificial neural network model. *Hydrogeol J* 20(8):1511–1527. <https://doi.org/10.1007/s10040-012-0894-7>
- Lee S, Hong SM, Jung HS (2018) GIS-based groundwater potential mapping using artificial neural network and support vector machine models: the case of Boryeong city in Korea. *Geocarto Int* 33(8): 847–861. <https://doi.org/10.1080/10106049.2017.1303091>
- Magesh NS, Chandrasekar N, Soundranayagam JP (2012) Delineation of groundwater potential zones in Theni district, Tamil Nadu, using remote sensing, GIS and MIF techniques. *Geosci Front* 3(2):189–196. <https://doi.org/10.1016/j.gsf.2011.10.007>
- Mageshkumar P, Subbaiyan A, Lakshmanan E, Thirumoorthy P (2019) Application of geospatial techniques in delineating groundwater potential zones: a case study from South India. *Arab J Geosci* 12(5): 151. <https://doi.org/10.1007/s12517-019-4289-0>
- Mogaji KA, Lim HS, Abdullah K (2015) Regional prediction of groundwater potential mapping in a multifaceted geology terrain using GIS-based Dempster-Shafer model. *Arab J Geosci* 8(5):3235–3258. <https://doi.org/10.1007/s12517-014-1391-1>
- Mukherjee I, Singh UK (2020) Delineation of groundwater potential zones in a drought-prone semi-arid region of east India using GIS and analytical hierarchical process techniques. *Catena* 194:104681. <https://doi.org/10.1016/j.catena.2020.104681>
- Mukherjee P, Singh CK, Mukherjee S (2012) Delineation of groundwater potential zones in arid region of India—a remote sensing and GIS approach. *Water Resour Manag* 26(9):2643–2672. <https://doi.org/10.1007/s11269-012-0038-9>
- Nag SK, Kundu A (2016) Application of remote sensing, GIS and MCA techniques for delineating groundwater prospect zones in Kashipur block, Purulia district, West Bengal. *Appl Water Sci* 8(1):38. <https://doi.org/10.1007/s13201-018-0679-9>
- Naghbi SA, Pourghasemi HR (2015) A comparative assessment between three machine learning models and their performance comparison by bivariate and multivariate statistical methods in groundwater potential mapping. *Water Resour Manag* 29(14):5217–5236. <https://doi.org/10.1007/s11269-015-1114-8>
- Naghbi SA, Pourghasemi HR, Dixon B (2016) GIS-based groundwater potential mapping using boosted regression tree, classification and regression tree, and random forest machine learning models in Iran. *Environ Monit Assess* 188(1):44. <https://doi.org/10.1007/s10661-015-5049-6>
- Nair HC, Padmalal D, Joseph A, Vinod PG (2017) Delineation of groundwater potential zones in river basins using geospatial tools—an example from southern western Ghats, Kerala, India. *J Geovisualization Spat Anal* 1(1-2):5. <https://doi.org/10.1007/s41651-017-0003-5>
- Nefeslioglu HA, Sezer EA, Gokceoglu C, Ayas Z (2013) A modified analytical hierarchy process (M-AHP) approach for decision support systems in natural hazard assessments. *Comput Geosci* 59:1–8. <https://doi.org/10.1016/j.cageo.2013.05.010>
- Nithya CN, Srinivas Y, Magesh NS, Kaliraj S (2019) Assessment of groundwater potential zones in Chittar basin, Southern India using GIS based AHP technique. *Remote Sens Appl Soc Environ* 15: 100248. <https://doi.org/10.1016/j.rsase.2019.100248>
- Palchaudhuri M, Biswas S (2020) Application of LISS III and MODIS-derived vegetation indices for assessment of micro-level agricultural drought. *Egypt J Remote Sens Space Sci* 23(2):221–229. <https://doi.org/10.1016/j.ejrs.2019.12.004>
- Pande CB, Khadri SFR, Moharir KN, Patode RS (2017) Assessment of groundwater potential zonation of Mahesh River basin Akola and Buldhana districts, Maharashtra, India using remote sensing and GIS techniques. *Sustain Water Resour Manag* 4:1–15. <https://doi.org/10.1007/s40899-017-0193-5>
- Parmar M, Shukla S, Kalubarme MH (2019) Impact of climate change and drought analysis on agriculture in Sabarkantha district using geoinformatics technology. *Glob J Eng Sci Res* 6(5):133–144. <https://doi.org/10.5281/zenodo.2751054>
- Patra S, Mishra P, Mahapatra SC (2018) Delineation of groundwater potential zone for sustainable development: a case study from Ganga Alluvial Plain covering Hooghly district of India using remote sensing, geographic information system and analytic hierarchy process. *J Clean Prod* 172:2485–2502. <https://doi.org/10.1016/j.jclepro.2017.11.161>
- Peters E, Torfs PJF, van Lanen HAJ, Bier G (2003) Propagation of drought through groundwater—a new approach using linear reservoir theory. *Hydrol Process* 17(15):3023–3040. <https://doi.org/10.1002/hyp.1274>
- Peters E, Van Lanen HAJ, Torfs PJF, Bier G (2005) Drought in groundwater—drought distribution and performance indicators. *J Hydrol* 306(1-4):302–317. <https://doi.org/10.1016/j.jhydrol.2004.09.014>
- Pfeiffer L, Lin CYC (2014) The effects of energy prices on agricultural groundwater extraction from the High Plains Aquifer. *Am J Agric Econ* 96(5):1349–1362. <https://doi.org/10.1093/ajae/aa020>
- Pourghasemi HR, Beheshtirad M (2015) Assessment of a data-driven evidential belief function model and GIS for groundwater potential mapping in the Koohrang Watershed, Iran. *Geocarto Int* 30(6):662–685. <https://doi.org/10.1080/10106049.2014.966161>
- Pourtaghi ZS, Pourghasemi HR (2014) GIS-based groundwater spring potential assessment and mapping in the Birjand Township, southern Khorasan Province, Iran. *Hydrogeol J* 22(3):643–662. <https://doi.org/10.1007/s10040-013-1089-6>
- Rahmati O, Samani AN, Mahdavi M, Pourghasemi HR, Zeinivand H (2014) Groundwater potential mapping at Kurdistan region of Iran using analytic hierarchy process and GIS. *Arab J Geosci* 8(9):7059–7071. <https://doi.org/10.1007/s12517-014-1668-4>
- Rahmati O, Haghizadeh A, Pourghasemi HR, Noormohamadi F (2016) Gully erosion susceptibility mapping: the role of GIS based bivariate statistical models and their comparison. *Nat Hazards* 82:1231–1258. <https://doi.org/10.1007/s11069-016-2239-7>
- Rajasekhar M, Sudarsana RG, Siddi RR (2019) Assessment of groundwater potential zones in parts of the semi-arid region of Anantapur District, Andhra Pradesh, India using GIS and AHP approach. *Model Earth Syst Environ* 5:1303–1317. <https://doi.org/10.1007/s40808-019-00657-0>
- Rajasekhar M, Gadhiraaju SR, Kadam A, Bhagat V (2020) Identification of groundwater recharge-based potential rainwater harvesting sites for sustainable development of a semi-arid region of southern India using geospatial, AHP, and SCS-CN approach. *Arab J Geosci* 13(2): 24. <https://doi.org/10.1007/s12517-019-4996-6>
- Razandi Y, Pourghasemi HR, Neisani NS, Rahmati O (2015) Application of analytical hierarchy process, frequency ratio, and certainty factor models for groundwater potential mapping using GIS. *Earth Sci Inf* 8(4):867–883. <https://doi.org/10.1007/s12145-015-0220-8>
- Rehman HU, Ahmad Z, Ashraf A, Ali SS (2019) Predicting groundwater potential zones in upper Thal Doab, Indus Basin through integrated use of RS and GIS techniques and groundwater flow modeling. *Arab J Geosci* 12(20):621. <https://doi.org/10.1007/s12517-019-4783-4>
- Rouse JW, Haas RH, Scell JA, Deering DW, Harlan JC (1974) Monitoring the vernal advancements and retrogradation (green wave effect) of nature vegetation. In: NASA/GSFC final report MD.371. NASA, Greenbelt.
- Roy S, Hazra S, Chanda A, Das S (2020) Assessment of groundwater potential zones using multi-criteria decision-making technique: a micro-level case study from red and lateritic zone (RLZ) of West

- Bengal, India. *Sustain Water Resour Manag* 6(1):4. <https://doi.org/10.1007/s40899-020-00373-z>
- Rudra K, Mukherjee SS, Mukhopadhyay UK, Gupta D (2017) State of environment report, West Bengal, 2016. Saraswati Press Ltd, West Bengal Pollution Control Board
- Saaty TL (1980) *The analytic hierarchy process: planning, priority setting, resource allocation*. McGraw Hill, New York
- Saaty TL (1990) How to make a decision: the analytic hierarchy process. *Eur J Oper Res* 48(1):9–26. [https://doi.org/10.1016/0377-2217\(90\)90057-I](https://doi.org/10.1016/0377-2217(90)90057-I)
- Saghebian SM, Sattari MT, Mirabbasi R, Pal M (2014) Ground water quality classification by decision tree method in Ardebil region, Iran. *Arab J Geosci* 7:4767–4777. <https://doi.org/10.1007/s12517-013-1042-y>
- Sargaonkar AP, Rathi B, Baile A (2011) Identifying potential sites for artificial groundwater recharge in sub-watershed of River Kanhan, India. *Environ Earth Sci* 62:1099–1108. <https://doi.org/10.1007/s12665-010-0598-z>
- Schaetzl RJ, (2013) Catenas and soils. In: Shroder, J. (Editor in Chief), Pope, G.A. (Ed.), *Treatise on geomorphology*. Academic Press, San Diego, CA, vol. 4, Weathering and Soils Geomorphology, pp 145–158. <https://doi.org/10.1016/b978-0-12-374739-6.00074-9>
- Senapati U, Das TK (2020) Assessment of potential land degradation in Akarsha Watershed, using GIS and multi-influencing factor technique. In: Shit P., Pourghasemi H., Bhunia G. (eds) *Gully erosion studies from India and surrounding regions*. *Advances in Science, Technology & Innovation (IEREK Interdisciplinary Series for Sustainable Development)*. Springer, Cham., pp 187–205. https://doi.org/10.1007/978-3-030-23243-6_11
- Shaban A, Khawlie M, Abdallah C (2006) Use of remote sensing and GIS to determine recharge potential zone: the case of Occidental Lebanon. *Hydrogeol J* 14(4):433–443. <https://doi.org/10.1007/s10040-005-0437-6>
- Shekhar S, Pandey AC (2015) Delineation of groundwater potential zone in hard rock terrain of India using remote sensing, geographical information system (GIS) and analytic hierarchy process (AHP) techniques. *Geocarto Int* 30(4):402–421. <https://doi.org/10.1080/10106049.2014.894584>
- Shen Y, Oki T, Utsumi N, Kanae S, Hanasaki N (2008) Projection of future world water resources under SRES scenarios: water withdrawal// Projection des ressources en eau mondiales futures selon les scénarios du RSSE: prélèvement d'eau. *Hydrol Sci* 53(1):11–33. <https://doi.org/10.1623/hysj.53.1.11>
- Shen Y, Oki T, Kanae S, Hanasaki N, Utsumi N, Kiguchi M (2014) Projection of future world water resources under SRES scenarios: an integrated assessment. *Hydrol Sci J* 59(10):1775–1793. <https://doi.org/10.1080/02626667.2013.862338>
- Tabor NJ, Myers TS, Michel LA (2017) *Sedimentologist's guide for recognition, description, and classification of Paleosols*. *Terr Depos Syst*:165–208. <https://doi.org/10.1016/b978-0-12-803243-5.00004-2>
- Tahmassebpour N, Rahmati O, Noomohamadi F, Lee S (2016) Spatial analysis of groundwater potential using weights-of-evidence and evidential belief function models and remote sensing. *Arab J Geosci* 9:79. <https://doi.org/10.1007/s12517-015-2166-z>
- Thapa R, Gupta S, Guin S, Kaur H (2017) Assessment of groundwater potential zones using multi-influencing factor (MIF) and GIS: a case study from Birbhum district, West Bengal. *Appl Water Sci* 7(7): 4117–4131. <https://doi.org/10.1007/s13201-017-0571-z>
- Thivya C, Chidambaram S, Tirumalesh K, Prasanna MV, Thilagavathi R, Nepolian M (2014) Occurrence of the radionuclides in groundwater of crystalline hard rock regions of central Tamil Nadu, India. *J Radioanal Nucl Chem* 302(3):1349–1355. <https://doi.org/10.1007/s10967-014-3630-z>
- Wang J, Rothausen SG, Conway D, Zhang L, Xiong W, Holman IP, Li Y (2012) China's water–energy nexus: greenhouse-gas emissions from groundwater use for agriculture. *Environ Res Lett* 7(1): 014035. <https://doi.org/10.1088/1748-9326/7/1/014035>
- White I, Falkland T, Scott D. (1999) *Droughts in small coral islands: case study, South Tarawa, Kiribati*. IHP-V, technical documents in hydrology, No.26.Paris:Unesco. http://www.bom.gov.au/water/about/waterResearch/document/White_et_al_IHPV_Report_26_1999.pdf. Accessed 6 April 2020
- Yeh HF, Cheng YS, Lin HI, Lee CH (2016) Mapping groundwater recharge potential zone using a GIS approach in Hualian River, Taiwan. *Sustain Environ Res* 26:33–43. <https://doi.org/10.1016/j.serj.2015.09.005>
- Zabihi M, Pourghasemi HR, Pourtaghi ZS, Behzadfar M (2016) GIS-based multivariate adaptive regression spline and random forest models for groundwater potential mapping in Iran. *Environ Earth Sci* 75(8):665. <https://doi.org/10.1007/s12665-016-5424-9>